

# Chapter 19

## One-, Two- and Three-Dimensional Pedogenetic Models

Uta Stockmann, Sebastien Salvador-Blanes, Tom Vanwalleghem,  
Budiman Minasny, and Alex. B. McBratney

*“We know more about the movement of celestial bodies than  
about the soil underfoot”.*

Leonardo da Vinci, circa 1500s

### 19.1 Modelling and Quantifying Pedological Processes

Various methods have been used to measure or estimate pedogenic processes that are responsible for the differentiation of a soil profile. The most important pedogenic processes can be seen in Fig. 19.1, in a simplified form.

In the following, the modelling and quantification of these processes will be reviewed and discussed, in particular transformation processes (soil physical and chemical weathering) and translocation processes (eluviation and illuviation and soil mixing).

---

U. Stockmann (✉) • B. Minasny • A.B. McBratney  
Sydney Institute of Agriculture & School of Life and Environmental Sciences,  
The University of Sydney, Sydney, NSW 2006, Australia  
e-mail: [uta.stockmann@sydney.edu.au](mailto:uta.stockmann@sydney.edu.au); [budiman.minasny@sydney.edu.au](mailto:budiman.minasny@sydney.edu.au);  
[alex.mcbratney@sydney.edu.au](mailto:alex.mcbratney@sydney.edu.au)

S. Salvador-Blanes  
Laboratoire Géo Hydrosystèmes Continentaux, Faculté des Sciences et Techniques,  
Parc de Grandmont, 37200 Tours, France  
e-mail: [salvador@univ-tours.fr](mailto:salvador@univ-tours.fr)

T. Vanwalleghem  
Departamento de Agronomía, Universidad de Córdoba, Córdoba, Spain  
e-mail: [ag2vavat@uco.es](mailto:ag2vavat@uco.es)

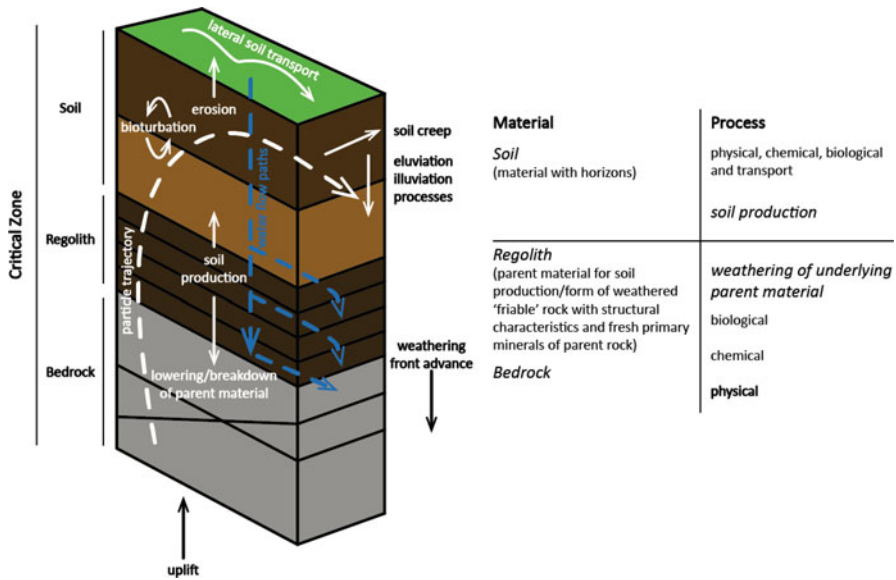


Fig. 19.1 Important pedogenic processes that are responsible for the differentiation of a soil profile (After Stockmann 2010)

### 19.1.1 Chronofunctions

Jenny’s (1941) *clorpt* model introduced in the previous chapter describes the relationship between soil properties and time. The term chronofunction is equated with the mathematical expression of chronosequence data representing a solution to Jenny’s state-factor equation (Yaalon 1975; Schaetzel et al. 1994). Jenny (in Stevens and Walker 1970) stated that if we know the ages and properties quantitatively, we have a chronofunction and can fit rate equations to the data; if the ages are relative, we have a chronosequence, from which we can learn a lot about processes and mechanisms, but not necessarily rates. Chronofunctions can perhaps be seen as nonstationary and to represent soil evolution from some non-equilibrium state to an equilibrium state.

Chronosequences are used to investigate and understand the formation of soil profiles, i.e. placing soil profiles developed from surfaces of known or dated age in a chronological order (Huggett 1998; Sauer et al. 2007). They can be used to formalize chronofunctions where soil and landscape properties are plotted against the independent variable time:

$$S(\text{Soil}) = f_t(\text{time}) \text{cl, o, r, p} \dots \tag{19.1}$$

If we believe soil formation is a result of predominantly chemical processes, we may expect the form of the chronofunctions to obey chemical models such

as zero-, first- or second-order kinetics (Sparks 1995). First-order kinetic models show an exponential evolution with time to some asymptotic value. One of the main parameters of this model is a rate constant which can give us estimates of the natural rate of soil formation.

Obtaining data for a chronosequence is not easy; following Jenny's factorial model, it may be impossible to achieve, i.e. finding a site with the same parent material, under ineffectively varying climatic conditions and influence of organisms, and constant relief. However, approximate chronofunctions with various assumptions can be obtained. In several parts of the world, volcanic activity, mudflows or glaciation has created surface materials or soil where the relative age can be determined. An example can be found on the Hawaiian Islands, with a sequence of volcanic surfaces that ranges in substrate age, from a currently active volcano (0 years) to the 4 million-year-old island of Kauai (Kitayama et al. 1997a, b). Kitayama et al. (1997a, b) chose an array of sites formed from basaltic lava parent material, with similar elevation about 1200 m above sea level with minimal topographic relief and a mean annual rainfall of 4000 mm. The island also has a uniform vegetation coverage with rain forests dominated by a single tree species.

Such chronosequences can be utilized in the calculation of the *surface age-profile thickness* (SAST) which represents the long-term average of soil formation (Egli et al. 2014). In a stable environment with minimal processes of erosion and deposition, soil formation rates are calculated from the thickness of the soil divided by the age of the surface soil (in mm/year or if density is considered in Mg/km<sup>2</sup>/year).

There are different types of mathematical functions that have been commonly used in chronofunctions, to express soil evolution with time, as exemplified in Fig. 19.2, with simple linear and logarithmic functions perhaps being the most frequently used. Jenny (1941) postulated that soil property change over time could be of sigmoidal shape with an initial exponential rate and that the changes gradually become small as they are reaching a steady-state condition (Yaalon 1975). Barrett and Schaetzl (1992) used a single logarithmic model to exemplify the change of the quantity of iron over time during podsolization for a sandy soil near Lake Michigan. Hay (1960) on the other hand found an exponential relationship between clay formation and time from volcanic ash on the island of St. Vincent in the Caribbean as would be expected from first-order kinetics.

### 19.1.2 Soil Weathering Models and Rates

The importance of soil and its genesis and therefore the quantification of processes of soil weathering are part of at least two of the nine *Grand Challenges in Earth Surface Processes* that has been put forward by the NRC (2010) publication. It specifically states that "The breakdown of bedrock – a major factor in Earth surface processes – is among the least understood of the important geological processes".

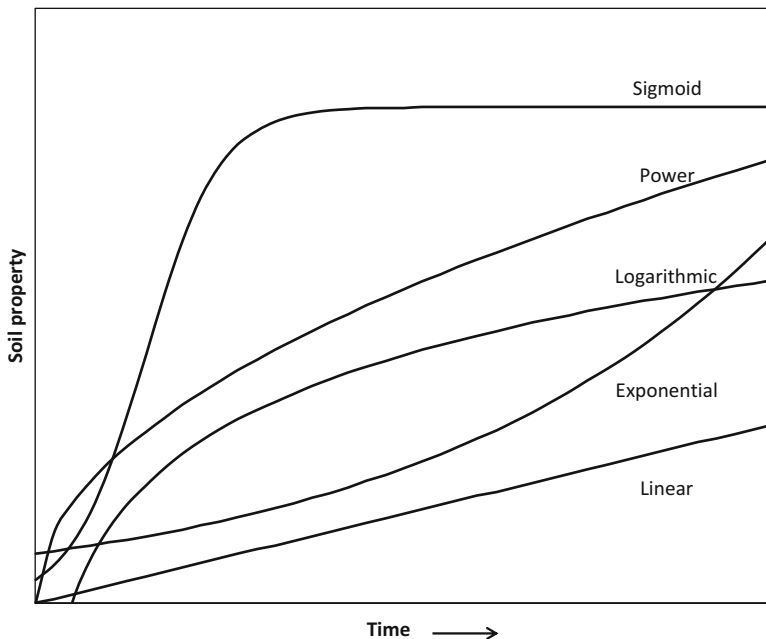


**Fig. 19.2** Types of mathematical functions commonly used in chronofunctions. S-shaped or sigmoidal curve, general form of equation,  $Y = 1/(a + b\exp(-t))$ ; power functions, general form of equation,  $Y = at^b$ ; logarithmic functions, general form of equation,  $Y = a + b(\log t)$ ; exponential functions, general form of equation,  $Y = a\exp(bt)$ ; simple linear functions, general form of equation,  $Y = a + bt$  (Stockmann 2010)

Over the years, geomorphologists and pedologists have attempted to formalize rates of soil production from parent materials which led to two assumed main concepts or models of soil weathering with time, the (1) *exponential soil production model* and the (2) *humped soil production model* (visualized in Fig. 19.3). The first states that soil production decreases exponentially with increasing thickness of the overlying soil mantle (Ahnert 1977; Heimsath et al. 1997), whereas the second model explains the conversion of rock into soil using a humped function where soil production is greatest below an incipient soil depth and slower for exposed bedrock or an already thick soil mantle (Gilbert 1877; Humphreys and Wilkinson 2007).

The first concept, the exponential decline of the soil production rate (SPR) with increasing soil depth, can be described as (Dietrich et al. 1995; Heimsath et al. 1997):

$$SPR = P_0 \exp(-bh) \tag{19.2}$$

where  $P_0$  ( $[L T^{-1}]$ , mm kyr<sup>-1</sup>) is the rate of weathering of bedrock at zero soil thickness ( $h$  ( $[L]$ , cm)) and  $b$  ( $[L^{-1}]$ , cm<sup>-1</sup>) is a rate constant, a length scale that

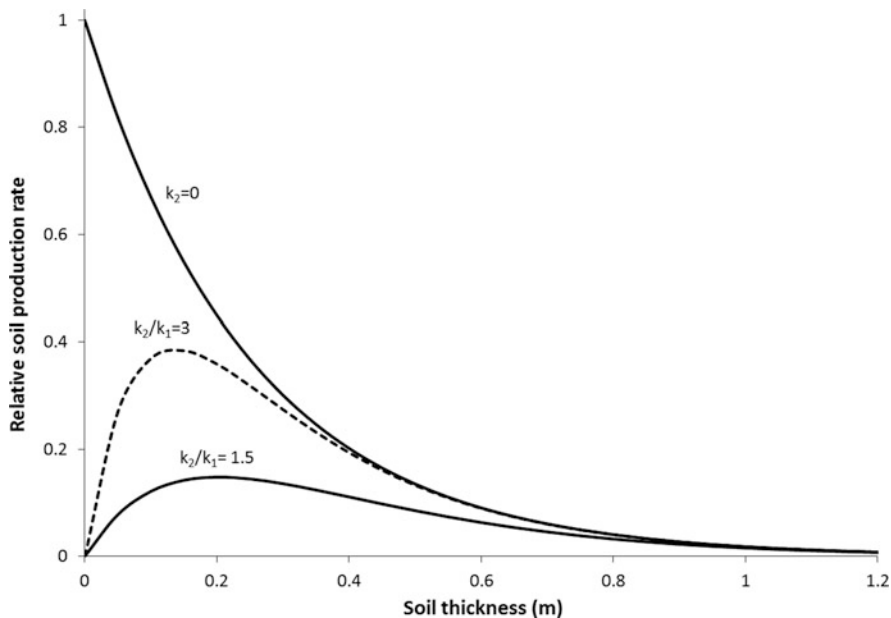


**Fig. 19.3** The rate of soil production versus soil thickness (based on Minasny and McBratney 2006; Furbish and Fagherazzi 2001). Here, both the exponential and the humped soil production models are presented. Both axes are dimensionless. Soil production is presented graphically depending on different values of the parameter  $k_1$  and  $k_2$  (also refer to Eqs. 19.3 and 19.4). If  $k_2 = 0$ , the soil production equals a depth-dependent exponentially decreasing soil production function. If  $k_2/k_1 \geq 0$ , soil production shows a humped function (changed after Stockmann et al. 2011)

characterizes the decline in soil production with increasing soil thickness. This model of soil production was first verified with field data from the Tennessee Valley in California, USA, by Heimsath et al. (1999), employing terrestrial cosmogenic nuclides (TCN).

The second concept, the humped model of soil production, can for example be formalized as a continuous double exponential function (Minasny and McBratney 2006):

$$\frac{\partial e}{\partial t} = - (P_0 [\exp(-k_1 h) - \exp(-k_2 h)] + P_a) \tag{19.3}$$

where  $P_0$  ( $[L T^{-1}]$ ,  $mm kyr^{-1}$ ) represents the rate of weathering of bedrock,  $h$  ( $[L]$ ,  $cm$ ) the soil thickness,  $k_1$  the rate of mechanical breakdown of the rock materials and  $k_2$  the rate of chemical weathering and  $P_a$  the weathering rate at steady-state condition ( $[L T^{-1}]$ ,  $mm kyr^{-1}$ ) with condition  $k_1 < k_2$ . When  $k_2$  equals 0, the humped function is reduced to the depth-dependent exponential soil production function (Eq. 19.2). The critical thickness,  $h_c$ , where weathering is at maximum is written as:

$$h_c = \frac{\ln(k_2/k_1)}{k_2 - k_1} \quad (19.4)$$

An empirical parameterization of the humped soil production model is still to be achieved, but this model was used to explain soil formation conceptually in some landscapes. Heimsath et al. (2009), for example, postulated that humped soil production occurred at their study site, Arnhem Land in northern Australia, an outcrop-dominated soil landscape where soil depths of less than the peak in soil production (35 cm) could not be observed. In a soil landscape dominated by humped soil production, it is assumed that soil depths less than the maximum in soil production are unstable and continuously eroded to expose the parent rock material (Dietrich et al. 1995).

### 19.1.2.1 Physical Weathering

#### Models of Physical Weathering

Physical weathering processes can be represented using different rock fragmentation models such as symmetric, asymmetric and Whitworth fragmentation and granular disintegration. Parent particles are weathered into daughter particles whilst preserving their mass based on these four different fragmentations which are shown graphically in Fig. 19.4 (Sharmeen and Willgoose 2006). Symmetric fragmentation weathers a parent particle into two daughter particles of equal volume; asymmetric fragmentation on the other hand results in two daughter particles of unequal volumes; Whitworth fragmentation results in a distribution of daughter particles proposed by W.A. Whitworth. Granular surface disintegration is a process used to model the particle breakdown of a thin surface layer which results in several equally sized spherical daughter particles that are of the same diameter as the thickness of the surface layer and one large daughter particle of equal diameter as the parent particle less twice the layer thickness (Wells et al. 2008).

Wells et al. (2008) modelled physical weathering based on these fragmentation models, including the probability of fragmentation to occur in a given time period. They found that the physical weathering rate increased linearly with time, based on the probability of fracture to occur. The Wells' fragmentation model was implemented by Welivitiya et al. (2016) for their soil-landscape model.

#### Quantifying the Rate of Physical Weathering

Several approaches have been utilized to parameterize weathering rates of parent material to soil from field data. Terrestrial cosmogenic nuclides, predominantly  $^{10}\text{Be}$ , have been employed to derive soil production rates of soil (Stockmann et al. 2014). In this method, soil production is interpreted as the physical conversion of bedrock into soil, which is usually expressed in mm of bedrock weathered over time

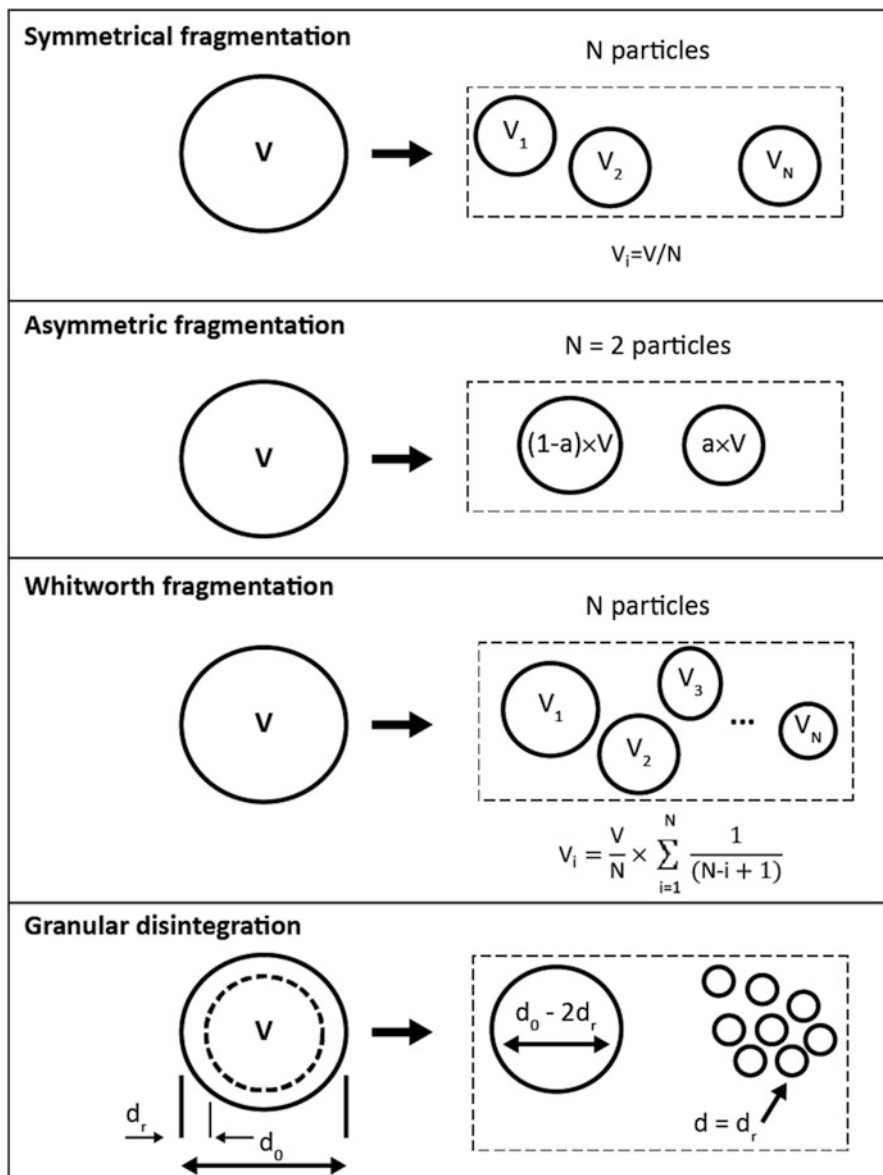


**Fig. 19.4** Fragmentation geometries used in the modelling of physical weathering; with  $V$  being the volume of a parent particle that fractures into  $N$  daughter particles ( $V_1, V_2$ , etc.),  $d$  the diameter of the parent particle,  $d_r$  the surface layer thickness of the parent particle and  $a$  the ratio of daughter particle volumes (Redrawn after Wells et al. 2008)

(mm kyr<sup>-1</sup>). For rate calculations, the rate  $P$  of <sup>10</sup>Be production in atoms g-quartz<sup>-1</sup> year<sup>-1</sup> at depth  $h$  and slope  $\theta$  (Stone 2000), the half-life of <sup>10</sup>Be in years (Chmeleff et al. 2009) and the concentration  $N$  of <sup>10</sup>Be in atoms g-quartz<sup>-1</sup> in the sample of interest (parent material) are required. Calculations are then based on a model by Nishiizumi et al. (1991) that allows for calculations of the steady-state concentration of <sup>10</sup>Be in the sample of interest. This model assumes that <sup>10</sup>Be concentrations are controlled by the increase of concentrations with exposure time and the erosion rate of the parent material itself ( $\varepsilon$  or SPR in cm year<sup>-1</sup>). Soil production rates in cm year<sup>-1</sup> or mm kyr<sup>-1</sup> can then be calculated by solving this model for SPR ( $\varepsilon$ ) (Lal 1991; Heimsath et al. 1997):

$$\text{SPR} = \frac{\Lambda}{\rho_{\text{parent}}} \left( \frac{P(h, \theta)}{N} - \lambda \right) \quad (19.5)$$

where  $\rho_{\text{parent}}$  is the mean density of the parent material in g cm<sup>-3</sup>,  $\lambda$  is the decay constant of <sup>10</sup>Be ( $\lambda = \ln 2 / ^{10}\text{Be}$  half-life) and  $\Lambda$  is the mean attenuation of cosmic rays (g cm<sup>-2</sup>). Annual production rates of <sup>10</sup>Be ( $P$ ) need to be normalized to the geographical position of the site studied (elevation, latitude and longitude) (Stone 2000); for soil-mantled landscapes, rates also need to be corrected for the soil overburden and shielding by slope (Dunne et al. 1999; Granger and Muzikar 2001). Soil production rates are calculated with the assumption of steady-state conditions where soil erosion and soil production rates are balanced throughout the production of TCN.

This technique was used in field studies situated in soil-mantled landscapes of Australia, North America and South America. Stockmann et al. (2014) compiled these measured rates of soil production which were as low as 0.0001 mm year<sup>-1</sup> and as high as 0.6 mm year<sup>-1</sup>, for soils of up to 108 cm of depth. These TCN field data were then used to derive for the first time a quantitative estimate of ‘global soil production’ with a rate of about 0.2 mm year<sup>-1</sup> (286 Mg km<sup>-2</sup> year<sup>-1</sup>). This rate reflects the potential weathering rate,  $P_0$ , for soil-mantled landscapes at zero soil depth (refer to Eq. 19.2). Such estimates are important for modelling global landscape dynamics, as we need to know the rate of soil replenishment from bedrock compared to its loss through erosion. This will be discussed a bit further in the concluding section of this chapter.

Uranium-series isotopes have also been used to estimate soil weathering or production rates (Dosseto et al. 2008). This technique assesses soil weathering throughout a soil profile based on the abundance of the U-series which is considered to be a function of chemical weathering and time and its distribution between primary and secondary minerals. In situ weathering can be identified (increase in weathering from the bottom to the top of a soil profile) through the decrease in the <sup>234</sup>U/<sup>238</sup>U ratios with decreasing soil depth. Soil residence times are then calculated by modelling the U-series activity ratios in a soil profile (Suresh et al. 2013). Research has shown that soil production rates derived with U-series isotopes



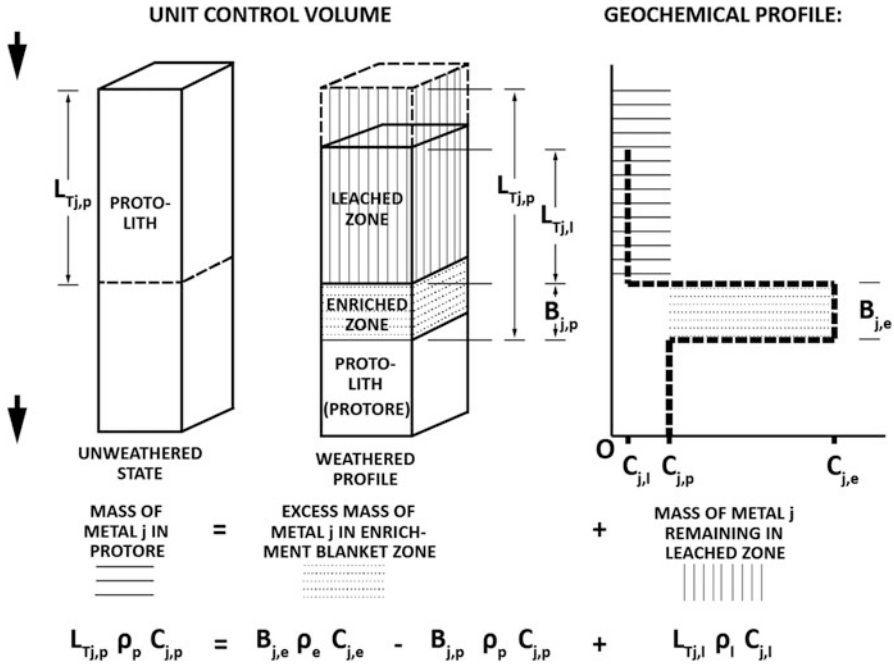


**Fig. 19.5** Graphical representation of one-dimensional mass balance for vertical supergene metal transport and secondary enrichment. The mass of element *j* leached is equal to the mass of *j* fixed in the underlying zone of secondary enrichment in this closed system model (with no lateral fluxes of loss of the element *j* through basal discharge) in which a protolith (*p*) volume becomes differentiated into two related parts. The uppermost subsystem is leached in element *j*, and the lower subsystem positioned further along a ground water flow line becomes enriched in *j*. Two strain terms are necessary. In the leached (*l*) zone,  $\epsilon_{j,l} = (L_{Tj,l} - L_{Tj,p})/L_{Tj,p}$ , and in the enriched (*e*) zone,  $\epsilon_{j,e} = (B_{j,e} - B_{j,p})/B_{j,p}$ , with *L* describing the thickness of the near-surface zone, *B* the thickness of the lower subset zone,  $\rho$  the density and *C* the concentration terms (Redrawn after Brimhall and Dietrich 1987)

are comparable to those derived from TCN (Dosseto et al. 2008; Suresh et al. 2013). Both methods therefore are quite robust to estimate soil production rates for soil-mantled hillslopes.

**19.1.2.2 Chemical Weathering**

Models of Chemical Weathering

Brimhall and Dietrich (1987) proposed a mass balance model that formally links chemical composition (of bedrock and soil) to bulk density, mineral density, volumetric properties, porosity and amount of deformation (strain). Figure 19.5 shows a graphical representation of such a chemical modelling approach.

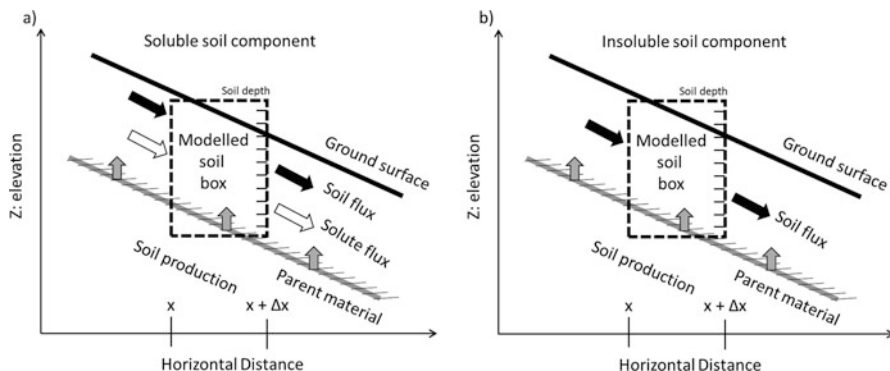


**Fig. 19.6** Mass fluxes on hillslope soils: (a) mass fluxes of soluble soil components in and out of a modelled soil box, (b) mass fluxes of an insoluble soil component in and out of a modelled soil box (Redrawn after Yoo et al. 2007)

Furthermore, Yoo et al. (2007) presented a process-oriented hillslope soil mass balance model that links processes of soil chemical weathering with topographic position (Fig. 19.6). The proposed model explicitly considers the influence of lateral soil transport and soil production from underlying bedrock (physical weathering) on soil chemical weathering processes.

### Quantifying the Rate of Chemical Weathering

The intensity of chemical weathering has been estimated from field-based studies through applying a variety of investigative methods. Chemical weathering rates have been estimated based on a mass balance approach, using elemental fluxes (loss and gain) in watersheds and the chemical composition of the parent materials and weathering products studied. Based on a compilation of studies reviewed in Stockmann et al. (2011), chemical weathering rates estimated from catchment-based mass loss of elements range between 0.01 and 0.1 mm year<sup>-1</sup> and are in general lower than rates of physical weathering (also refer to Fig. 19.7).

For a catchment, chemical fluxes can be estimated using a mass balance approach, by determining the solute discharge flux  $Q_{i,dis}$  for a chemical species  $i$ :

$$Q_{i,dis} = C_{i,dis} \frac{V}{At} \quad (19.6)$$

where  $C_{i,dis}$  is the chemical concentration of a chemical species  $i$ ,  $V$  is the fluid mass,  $A$  is the geographic area of the watershed and  $t$  is time (White and Blum 1995).

The chemical soil weathering rate ( $W$ ) can also be calculated in situ from the ratio of a resistant or immobile element (e.g. Zr) in the parent rock ( $[Zr]_{rock}$ ) as compared to its amount in the weathered rock (saprolite) or soil ( $[Zr]_{soil}$ ) (Riebe et al. 2004a, b):

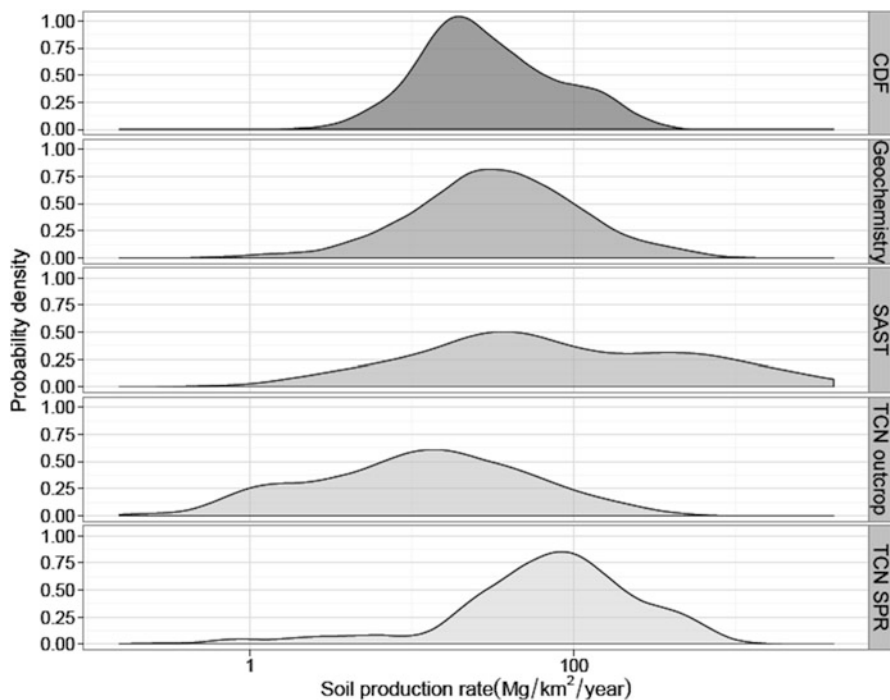


**Fig. 19.7** Probability density of soil formation rates in  $\text{Mg km}^{-2} \text{ year}^{-1}$  as reported by different methods. Note axes are in logarithmic scale, refer to Table 19.1 for data sources (Source: Minasny et al. 2015)

$$\frac{W}{D} = 1 - \frac{[\text{Zr}]_{\text{rock}}}{[\text{Zr}]_{\text{soil}}} = \text{CDF} \quad (19.7)$$

where CDF is the chemical depletion fraction which equals the ratio of the chemical weathering rate ( $W$ ) to the total denudation rate ( $D$ ). Soil weathering rates are often defined with different underlying assumptions. In a range of studies that used weathering ratios, total rates of denudation or weathering ( $D$ ) were substituted with rates of soil production derived from TCN (Riebe et al. 2003, 2004a, b; Green et al. 2006; Burke et al. 2007, 2009; Yoo et al. 2007). Some studies, however, considered soil production rates determined by TCN as rates of physical weathering only and subsequently added those to chemical weathering rates to calculate total denudation rates ( $D$ ) (Dixon et al. 2009).

The conservation of mass equation for the chemical weathering rate ( $\text{Mg km}^{-2} \text{ year}^{-1}$  or  $\text{mm year}^{-1}$ ) can be written as a fraction of the total denudation rate:

$$W = D \left( 1 - \frac{[\text{Zr}]_{\text{rock}}}{[\text{Zr}]_{\text{soil}}} \right) \quad (19.8)$$

The amount of chemical weathering can also be expressed for the loss of a specific element  $X$  (e.g. main base cations found in the soil such as Ca, Mg, K and Na) (Riebe et al. 2004a):

$$W_x = \left( [X]_{\text{rock}} - \frac{[Zr]_{\text{rock}}}{[Zr]_{\text{soil}}} \right) - [X]_{\text{soil}} \quad (19.9)$$

Stockmann et al. (2011) also compiled rates of chemical weathering derived from weathering indices and found that rates vary between 0 and 0.144 mm year<sup>-1</sup>. Rates derived with this method were relatively similar to rates derived from catchment-based mass balance studies, although overall rates derived from weathering indices were comparatively lower.

### 19.1.2.3 Conclusions: How Fast Does Soil Form?

As discussed in the previous sections, various field estimates are now available that can provide a quantitative measure of how fast soils form in the landscape. Minasny et al. (2015) compiled such rates in their recent publication that discusses how our world soils shape the landscape (Fig. 19.7). Soil weathering rates from different data sources are compared using the median of the distributions (see Table 19.1 for more details). This statistical measure was used as it is more representative of the distributions which tended to be skewed. Here, weathering rates were reported in units of mass of material over an area over time (Mg km<sup>-2</sup> year<sup>-1</sup>). Common bulk densities for rock (2600 kg m<sup>-3</sup>) and soil (1200 kg m<sup>-3</sup>) were used to convert volume (mm year<sup>-1</sup>) to mass for those studies where these were unknown. In the following, the amount of soil produced during weathering is discussed.

Figure 19.7 shows soil weathering rates derived from stable rock outcrops using the TCN technique (global median of 12 Mg km<sup>-2</sup> year<sup>-1</sup> or 10 mm kyr<sup>-1</sup>), and it becomes apparent that those are half to almost one order of magnitude smaller than soil production rates derived with TCN for soil-mantled landscapes (global median of 73 Mg km<sup>-2</sup> year<sup>-1</sup> or 60 mm kyr<sup>-1</sup>). This confirms general assumptions that terrain and environmental factors make a big difference for the intensity of weathering processes. For example, in general the presence of regolith (or partially weathered rock) is a precondition for intense weathering. Regolith or shallow soil mantles form a habitat for fauna and flora, and their presence also enhances the physical and chemical weathering rate. Figure 19.7 also shows that chemical weathering rates based on weathering ratios (global median of 24 Mg km<sup>-2</sup> year<sup>-1</sup> or 20 mm kyr<sup>-1</sup>) and chemical weathering rates based on river geochemistry (global median of 34 Mg km<sup>-2</sup> year<sup>-1</sup> or 28 mm kyr<sup>-1</sup>) are of similar value. Both are about a third of soil production rates derived from TCN.

However, we do not only need to know how fast our soils can form but also how much soil comparatively is lost through processes of erosion. In Fig. 19.8 average soil production rates for soil-mantled landscapes estimated from TCN field data are

**Table 19.1** Statistical distribution of soil production and weathering rates ( $\text{Mg km}^{-2} \text{ year}^{-1}$ ) from datasets derived using different measurement techniques

Percentile		SAST <sup>a</sup>	Terrestrial cosmogenic nuclide SPR <sup>b</sup> (0–100 cm)	Terrestrial cosmogenic nuclide on rock outcrop <sup>c</sup>	Chemical weathering based on river geo-chemistry <sup>d</sup>	Chemical weathering based on CDF <sup>e</sup>
100%	Maximum	4021	934	349	570	263
95%		1606	457	130	197	159
75%	Quartile	338	150	33	72	53
50%	Median	55	73	12	34	24
25%	Quartile	22	35	4	16	15
5%		4	4	1	6	5
0%	Minimum	1	0.3	0	1	0
	n	179	291	530	127	155

Source: Minasny et al. (2015)

<sup>a</sup>SAST Surface age-profile thickness (Data from Egli et al. 2014)

<sup>b</sup>SPR Soil production rate (Data from Stockmann et al. 2014 combined with Riebe et al. 2004a)

<sup>c</sup>Data from Portenga and Bierman (2011)

<sup>d</sup>Compiled data from Stockmann et al. (2014)

<sup>e</sup>Data from Riebe et al. (2004a) and compilation of Larsen et al. (2014), CDF chemical depletion fraction

therefore compared with erosion rates from different sources and scales. It becomes clear that rates and spatial patterns of erosion and deposition depend strongly on the type of erosion processes. For example, in natural environments that exhibit a dense vegetation cover, soil redistribution is mainly driven by mass wasting processes. In this regard, Fig. 19.8 illustrates that soil erosion rates under native vegetation (B) are comparatively low (global median of  $0.01 \text{ mm year}^{-1}$  equivalent to  $0.1 \text{ t ha}^{-1}$ ) and are in fact in a steady state with soil production rates (A) (global median of  $0.06 \text{ mm year}^{-1}$  equivalent to  $0.7 \text{ t ha}^{-1}$ ). Soil erosion, however, has been highly accelerated by human impact as anthropogenic land use changes and subsequently agricultural management practices have upset the natural balance between soil production and erosion. With a global median of  $2 \text{ mm year}^{-1}$  (equivalent to  $24 \text{ t ha}^{-1}$ ), soil erosion rates from conventionally managed agricultural soils (D) are almost two orders of magnitude higher than soil production rates (A). This shows that under humanly managed systems, soil does not seem to be a renewable resource and needs to be managed carefully. Changes in management practices towards more sustainable agricultural systems, where appropriate, however, can narrow the gap between soil production and humanly induced erosion rates. As seen in Fig. 19.8, erosion rates under conservation agricultural practices (C) are significantly reduced (global median of  $0.1 \text{ mm year}^{-1}$  equivalent to  $1.2 \text{ t ha}^{-1}$ ) and are close to a natural balance.

However, not all eroded soil material is actually lost in the streams as lateral transport through soil erosion is also an important mechanism for reshaping the

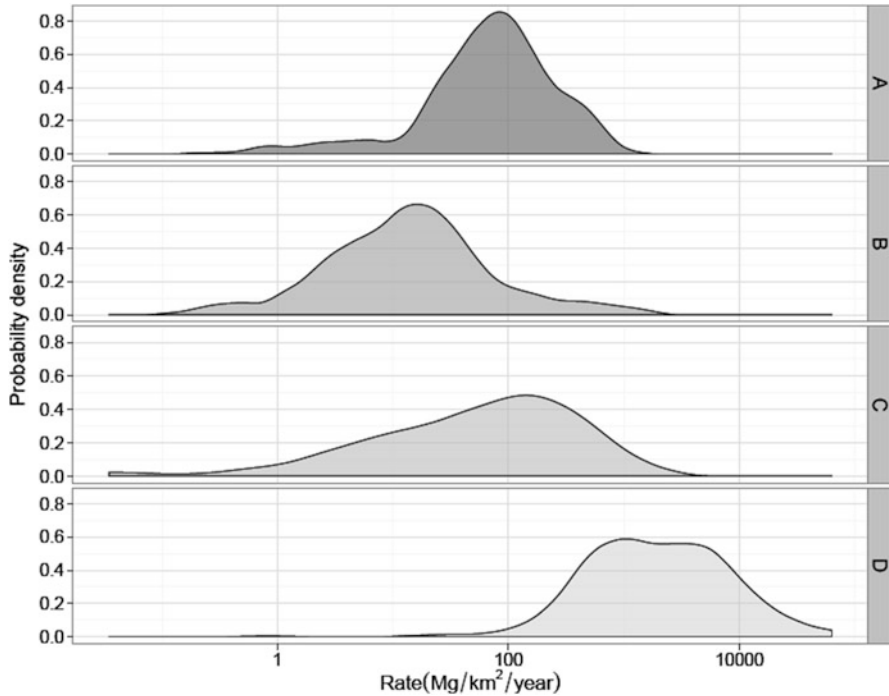


**Fig. 19.8** Statistical distribution of average soil production and erosion rates in  $\text{Mg km}^{-2} \text{ year}^{-1}$  from different sources and scales. **(a)** Soil production rates determined with TCN, **(b)** Erosion rate of native vegetation, **(c)** Erosion rate of conservation agriculture and **(d)** Erosion rate of conventional agriculture. TCN Soil production rate data are from Stockmann et al. (2014) and Riebe et al. (2004a). Erosion rates from conventional or conservation agriculture and native vegetation are from Montgomery (2007) (Source: Minasny et al. (2015))

Earth's surface through the redistribution of soil material and sediment in the landscape. Estimates of sediment delivery rates to streams, i.e. rates of actual loss of soil to the rivers and oceans, are therefore also needed to assess soil formation and soil transport in the landscape which is still a field that requires more work. Only a few estimates exist in the current literature. The rate of redistribution of soil and sediment to the land surface was estimated, for example, to be of a value of approximately  $1.11 \text{ mm year}^{-1}$  (Ludwig and Probst 1998). However, much lower estimates of about  $0.028 \text{ mm year}^{-1}$  (Syvitski et al. 2005) or much higher estimates of about  $12.6 \text{ mm year}^{-1}$  (Wilkinson and McElroy 2007) have also been reported in the literature on this topic.

### 19.1.3 Models of Soil Mixing

#### 19.1.3.1 Lessivage

##### Models of Clay Migration

The works of Van Wambeke in the 1970s are a first attempt to quantify lessivage, the translocation of clay particles during soil profile development (e.g. Van Wambeke 1972, 1976). In his 1976 paper, Van Wambeke (1976) proposed a mathematical model for the differential movement of clay particles which provides a quantitative expression of the pedological process of clay eluviation and illuviation. The quantification of clay migration through a soil profile is based on the assumption that the moving clay fraction which accumulates in the B horizon is associated with fine clay particles and that larger crystals ( $>0.2 \mu\text{m}$ ) are translocated more slowly through the profile or not at all. These translocation processes alter the ratio of fine clay ( $0\text{--}0.2 \mu\text{m}$ ) to total clay content ( $0\text{--}2 \mu\text{m}$ ) in the A and B horizons which can then be used as quantitative measure for the intensity of clay migration through the soil profile. These assumptions are only true however in a closed system without the removal, destruction, weathering, formation or addition of soil minerals, with constant horizon thicknesses and where no processes of erosion occur.

##### Quantifying Clay Migration

Radionuclides that are strongly adsorbed to the clay fraction and organic matter can be used to track their movement down the soil profile (He and Walling 1996; Zapata 2003).  $^{210}\text{Pb}$  and  $^{137}\text{Cs}$  that exhibit a half-life of 22.3 years and 30.2 years, respectively, can be used to investigate short-term vertical processes of soil translocation. These are moving passively down the soil profile using soil particles as carrier substances.

$^{210}\text{Pb}_{\text{ex}}$  is a product of the  $^{238}\text{U}$  decay series originating from the decay of gaseous  $^{222}\text{Rn}$ , a daughter radionuclide of  $^{226}\text{Ra}$ .  $^{226}\text{Ra}$  is found naturally in the soil and generates  $^{210}\text{Pb}$  which is usually in equilibrium with its parent  $^{226}\text{Ra}$ . Diffusion of small amounts of  $^{222}\text{Rn}$  introduces  $^{210}\text{Pb}$  into the atmosphere, and the fallout of this quantity of  $^{210}\text{Pb}$  on the soil surface is termed the excess  $^{210}\text{Pb}$  (hence  $^{210}\text{Pb}_{\text{ex}}$ ) that can be used to investigate its passive distribution through the soil profile. Dörr (1995) used  $^{210}\text{Pb}_{\text{ex}}$  to quantify the movement of organic matter and clay particles in forest soils, whereas Jagercikova et al. (2014) used  $^{210}\text{Pb}_{\text{ex}}$  to quantify clay migration under different farming practices.

Different to  $^{210}\text{Pb}$  which is a naturally occurring radionuclide,  $^{137}\text{Cs}$  stems from fallout of nuclear weapon tests (1950s to the 1970s) and accidents (e.g. Chernobyl, Ukraine, in 1986), and its accumulation in the surface soil can therefore be dated quite accurately, but its concentration in the world soils is also diminishing

following these fallout events. Because of its radioactive decay,  $^{137}\text{Cs}$  will not be available in the near future to be used in particle migration studies (Mabit et al. 2008).

### 19.1.3.2 Bioturbation

#### Models of Bioturbation

Gabet et al. (2003) reviewed quantitative models of bioturbation and sediment transport. They proposed a general slope-dependent model to calculate the horizontal volumetric flux of sediment ( $q_{sx}$ ) caused by root growth and decay:

$$q_{sx} = \frac{(x\tau r)}{(\rho_r)} \quad (19.10)$$

where  $x$  (m) is the net horizontal displacement of soil,  $r$  ( $\text{kg m}^{-2}$ ) is the root mass per unit area,  $\tau$  ( $\text{year}^{-1}$ ) is the root turnover rate which is a measure of the annual belowground production to the maximum belowground standing biomass and  $\rho_r$  ( $\text{kg m}^{-3}$ ) is the density of the root material. This model was used to derive estimates of sediment flux by root growth and decay for temperate grasslands ( $2.1 \times 10^{-4} \text{ m}^{-2} \text{ year}^{-1}$ ), sclerophyll shrubs ( $6.8 \times 10^{-4} \text{ m}^{-2} \text{ year}^{-1}$ ) and temperate forests ( $8.8 \times 10^{-4} \text{ m}^{-2} \text{ year}^{-1}$ ). Gabet et al. (2003) also formalized the horizontal alteration of soil along a hillslope caused by tree throw based on uphill and downhill mound building:

$$x_n = \bar{x}_d - \bar{x}_u = \frac{2}{\pi} (W + D) \sin \theta \quad (19.11)$$

where  $x_n$  is the long-term net horizontal transport distance (Eq. 19.11),  $x_d$  the horizontal distance of displacement of the root plate centroid caused by trees that were falling directly upslope (Eq. 19.13),  $x_u$  the horizontal distance of displacement of the root plate centroid caused by trees that were falling directly uphill (Eq. 19.12),  $W$  the width of the root plate and  $D$  the depth of the excavated pit.

$$x_u = \frac{W}{2} (\cos \theta - \sin \theta) - \frac{D}{2} (\cos \theta + \sin \theta) \quad (19.12)$$

$$x_d = \frac{W}{2} (\cos \theta + \sin \theta) + \frac{D}{2} (\cos \theta - \sin \theta) \quad (19.13)$$

Following on, Gabet and Mudd (2010) proposed a numerical model on bedrock erosion by root fracture and tree throw. Tree throw and associated processes of pit excavation and mound building that are responsible for the large-scale topography at the soil surface are modelled implementing concepts from the 2003 paper



(e.g. Eq. 19.11= $x_n$ ). Other processes, such as the fill in of the soil pits and flattening of the mounds that occur on smaller scales, are represented through slope-dependent processes of soil creep which is modelled through simple linear diffusion:

$$q_{sc} = DS \quad (19.14)$$

where  $q_{sc}$  ( $m^2 \text{ year}^{-1}$ ) is the sediment flux,  $D$  ( $m^2 \text{ year}^{-1}$ ) is the diffusivity and  $S$  ( $m \text{ m}^{-1}$ ) is the local slope.

This coupled biogeomorphic model is driven by field data from the Pacific Northwest (USA) on conifer population dynamics, rootwad volumes, tree throw frequency and soil creep. Model outcomes show a humped soil production relationship between bedrock erosion through biota and developing soil thickness. This relates to the principle that as the soil thickens, it becomes less likely for tree roots to disrupt the bedrock through weathering and that the growing soil medium provides a more favourable habitat for trees.

In this regard, recently, Shouse and Phillips (2016) investigated the effects of parent material on the biomechanical process of deepening of soils by trees. Especially the deepening of shallow soils is affected by this process of root penetration of parent material rocks. Two kinds of tree habitable bedrock were assessed in this study in comparison to adjacent non-tree sites, dipped and contorted rock with plenty of joints and bedding planes accessible for tree roots and flat level-bedded sedimentary rock. This study found that soils beneath tree stumps were significantly deeper, and the authors concluded that soil deepening effects through trees are an important mechanism under both easy and not so easily root accessible lithologies.

### Quantifying the Rate of Bioturbation

Radionuclides and also the technique of optically stimulated luminescence (OSL) have been used for ‘particle tracking’ within the soil profile and thus for generating rates of soil mixing. OSL is a dating technique that measures the time since soil particles (usually sand-sized grains) have been last exposed to sunlight before burial in the soil (Aitken 1998). A burial age in years for individual grains can be calculated using the dose ( $D_e$  in Gy,  $1 \text{ Gy} = 1 \text{ J kg}^{-1}$ ) the grains accumulated since burial, together with the annual dose rate ( $D_r$  in  $\text{Gy year}^{-1}$ ) the site studied receives:

$$\text{Burial age} = \frac{D_e}{D_r} \quad (19.15)$$

For example, Wilkinson and Humphreys (2005) and Stockmann et al. (2013) used OSL to investigate rates of soil mixing of forest soils, whereas Kaste et al. (2007) employed the short-lived radionuclides  $^7\text{Be}$  originating from cosmic radiation and the fallout radionuclide  $^{210}\text{Pb}_{\text{ex}}$  to explore rates of soil bioturbation.

## 19.2 Soil Profile Models

Pedologists have long been studying soils in many different environments to understand their distribution in the landscape (Dijkerman 1974). The basis for these studies is an approach at the pedon scale. These studies have allowed a good understanding of soil genesis processes, conducting to conceptual models of soil formation. These conceptual models that were discussed in Chap. 18 have in particular been of great use for soil mapping. But the major challenge for pedologists is to develop quantitative techniques, to be able to communicate their qualitative understanding of soil evolution to other disciplines (Hoosbeek 1994). Indeed, whereas other compartments of the ecosystem are quite well addressed, the soil seen as a whole entity was and still is often seen as a black box by non-pedologists (Wagenet et al. 1994).

On the other hand, many studies in the last decades have allowed a reasonably good understanding of individual soil processes, whether physical (e.g. heat transport, water movement, physical breakdown), chemical (e.g. ion exchange) or mineralogical (e.g. mineral dissolution). These studies are of great importance to understand the fate of solid and dissolved matter in the soils in specific situations, but do not directly address our approach. The PROFILE biogeochemical model (Sverdrup and Warfvinge 1993) is one of the attempts to integrate sub-models into a single operational model. The focus has been put exclusively on biogeochemical changes and transfer of dissolved matter at the profile scale, generally for short timescales. This model is of major importance to quantify the evolution of soils in particular in response to present human activities (e.g. critical loads), but reflects only partially the evolution of soils, as it does not take into account, for example, the evolution of particle size.

There is therefore a great need to develop an interdisciplinary approach (Brantley et al. 2011) to allow a connection between these processes to integrate them in a single global model, with a pedologic perspective (Levine and Knox 1994). This modelling at the profile scale would moreover be a possibility to test our understanding of soil formation from the incipient stages (Oreskes et al. 1994; Heuvelink and Webster 2001).

The mechanistic modelling of soil formation encounters several difficulties:

- *The variation of the factors of soil formation over the timescale of soil formation, affecting the rate of the processes, but as well the processes themselves of soil formation:*
  - Variation of climate conditions in the past and the difficulty to reconstruct those
  - Changes in soil genesis processes occurring over time, e.g. changes in land use at the Holocene, recent mechanization (Sommer et al. 2008), changes in vegetation due to climate changes or changes in soil properties, etc.

- The integration of processes into a single model when the level of temporal resolution is not the same (e.g. organic matter input and decay vs. particle size evolution)
- *A good knowledge of the modelling of some processes (in particular biogeochemical processes), but a limited knowledge for others (e.g. bioturbation, clay migration, physical fractionation).*
- *A difficulty to validate these models due to the large temporal scales involved.* One of the solutions proposed is to work specifically on chronosequences which we discussed in the previous chapter.

Only a few studies have emerged to address this purpose since the founding theoretical work developed by Kirkby (1977). Two approaches can be envisaged: using existing sub-models and merging them in a single soil profile model or modelling soil profile evolution using simple equations that limit the number of input parameters with the aim to remain sufficiently generic and simple. An illustration of the first approach is the work performed by Finke and Hutson (2008) and Finke (2012). They model the evolution of soils from loose parent material by integrating two existing sub-models (focusing on carbon dynamics and biogeochemistry, respectively) and adding new soil formation processes. The second approach can be illustrated by the work performed by Salvador-Blanes et al. (2007), where soils developed from hard bedrock and are modelled using as a basis the work performed by Minasny and McBratney (1999, 2001).

### ***19.2.1 The Founding Work of M. J. Kirkby***

Kirkby (1977, 1985) developed the first comprehensive mathematical model of soil profile evolution. The basis for the soil profile modelling is here to consider the ‘proportion  $p$  of substance remaining’ at any depth, the value of  $p$  approaching 1 asymptotically at depth. In this model, there is no assumption about the exact limit between soil and unweathered parent material. Processes such as change in the bulk density of the soil, physical translocation of clays and particle size evolution are discarded.

Three sub-models with different timescales are considered: organic matter, nutrient cycling and the weathering profile. In situ processes linked with these sub-models comprise nutrient uptake, organic matter input and decay through leaf-fall, nutrient cycling, mixing of the topsoil, solute transfer through leaching and ionic diffusion. A mechanical denudation rate, introducing geomorphic processes, is as well considered. The soil chemistry is simplified to integrate all processes at once and in a geomorphic perspective.

### **19.2.1.1 Percolation**

The percolation process is modelled as an annual flow proportional to the pore-space available, the latter being considered as equal to the accumulated deficit of weathered material. Annual evapotranspiration and total rainfall are specified as input parameters. Evapotranspiration is a function of the distribution of roots that follows an exponential decay with soil depth. This distribution is considered as constant in the model. The amount of water percolating at any depth is a function of rainfall less evapotranspiration.

### **19.2.1.2 Solubility**

A key issue for modelling the solubility of the mineral constituents is that thermodynamic equilibrium between solutes and soil composition is assumed: the water residence times are considered long enough to approach equilibrium. The mineral constituents of soils are simplified and considered as a mixture of their constituent oxides. These dissolve independently to create ions, using Gibbs free energy values that are empirically adjusted by comparing the values for the minerals and the sum of those values considering their constituent oxides. Weathering at a given soil depth is a function of the quantity of water passing through, combined with values of partial pressure of CO<sub>2</sub> linked with the vegetation cover. Simulations show that soils formed from various parent materials are all eventually enriched in sesquioxides after a variable duration. Both the vegetation and the climate component are strongly affecting the degree of weathering through the partial pressure of CO<sub>2</sub> and the accumulated flow, respectively.

### **19.2.1.3 Leaching**

The leaching process is only considered for the inorganic profile. As for the organic profile, nutrients are only released through decomposition. The total solute concentration in the inorganic profile for a given proportion of substance remaining is considered as equivalent to the product of the difference in concentration of inorganic materials relative to the weathering profile and their solubility.

### **19.2.1.4 Ionic Diffusion and Organic Mixing**

Ionic diffusion allows a redistribution of solutes in the soil profile, proportionally to the concentration gradient. It is a key process in areas where the flow of water is very low to allow weathering, especially close to the unweathered bedrock. The ionic diffusion coefficient is here defined as a function of the porosity of the soil.

The organic mixing process is modelled as a diffusion process of soil material through the burrowing activity of the soil fauna. It decreases exponentially with depth. Therefore, while organic mixing is a dominant process close to the surface, ionic diffusion is dominant at depth.

### **19.2.1.5 Nutrient Uptake, Leaf-Fall and Organic Matter Decomposition**

Inorganic nutrients are supplied to plants through evapotranspiration, without considering seasonal variations. The total uptake of a nutrient is approached as the product of the ion concentration and of evapotranspiration rate. These nutrients are considered to be taken only from the inorganic part of the soil. The model considers that there is a constant proportion of plant biomass that falls annually. Only aboveground biomass input is considered. An equilibrium rate balancing uptake is reached over 25 years in the model. Organic matter decomposition rates are considered as constant for a given climate, whatever the organic matter composition. This rate is set at  $0.2 \text{ a}^{-1}$  for a climate with a mean annual temperature of  $10 \text{ }^{\circ}\text{C}$ .

The equations of these processes are combined whenever relevant in the three sub-models: organic matter, nutrient cycling and the weathering profile. The simulations performed allow producing more or less thick soils, organic-enriched topsoil, base-depleted topsoils in aridic conditions and more or less base-depleted intermediate horizons (root uptake activity) with a base-rich topsoil in humid conditions.

This pioneering work is the first attempt for the development of a comprehensive model of soil profile evolution. However, no further work derived from this initial attempt.

## **19.2.2 The Pedogen Model**

Salvador-Blanes et al. (2007, 2011) designed the Pedogen model of soil formation at the profile scale. The aim here was an attempt to translate the pedologist's approach – corresponding to a general phenomenological model – to a quantitative model of the key soil genesis processes. The idea is here to quantitatively model the transformation of a hard rock into soil material at the profile scale through various pedological processes that result in mineralogical transformations, organic matter input and decay and the translocation of solid or dissolved matter. In that respect, the model focuses on physical and chemical weathering, bioturbation, organic matter input and decay (Figs. 19.9 and 19.10) and on the retroactions between these processes with time steps of several decades to centuries that require simplifications in the processes modelled.

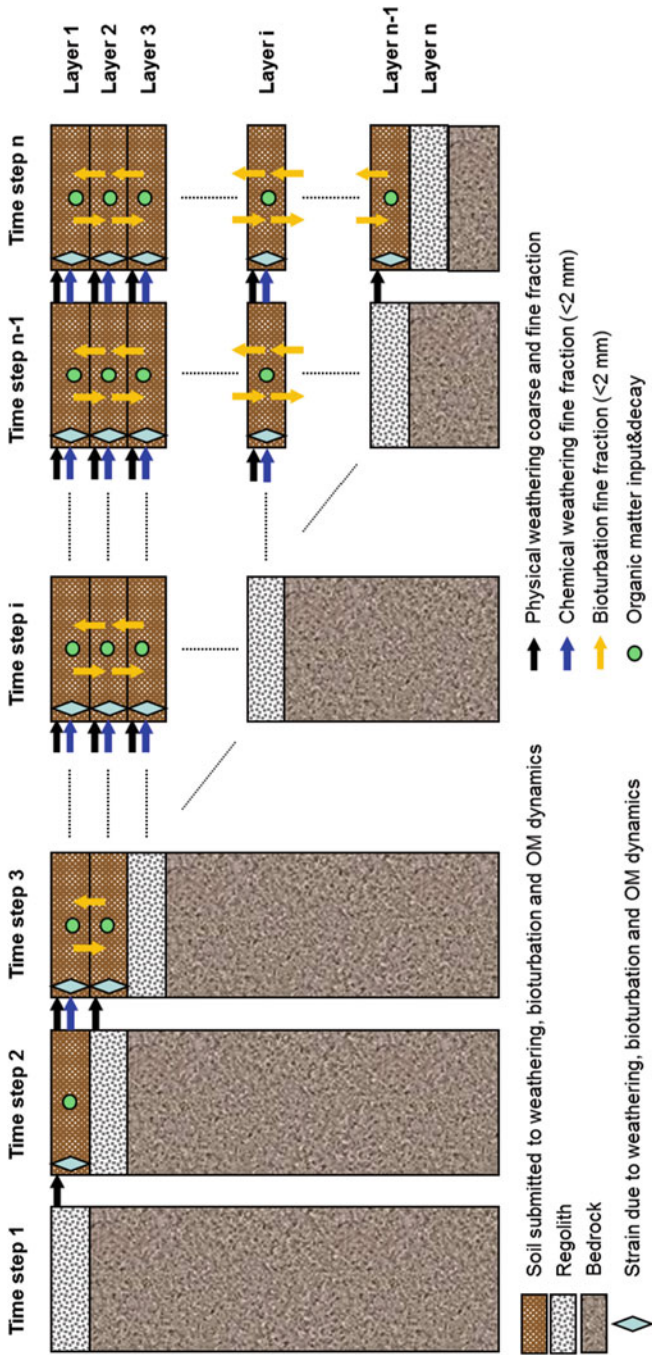


**Fig. 19.9** Structure of the Pedogen model (After Salvador-Blanes et al. 2007, used with permission)

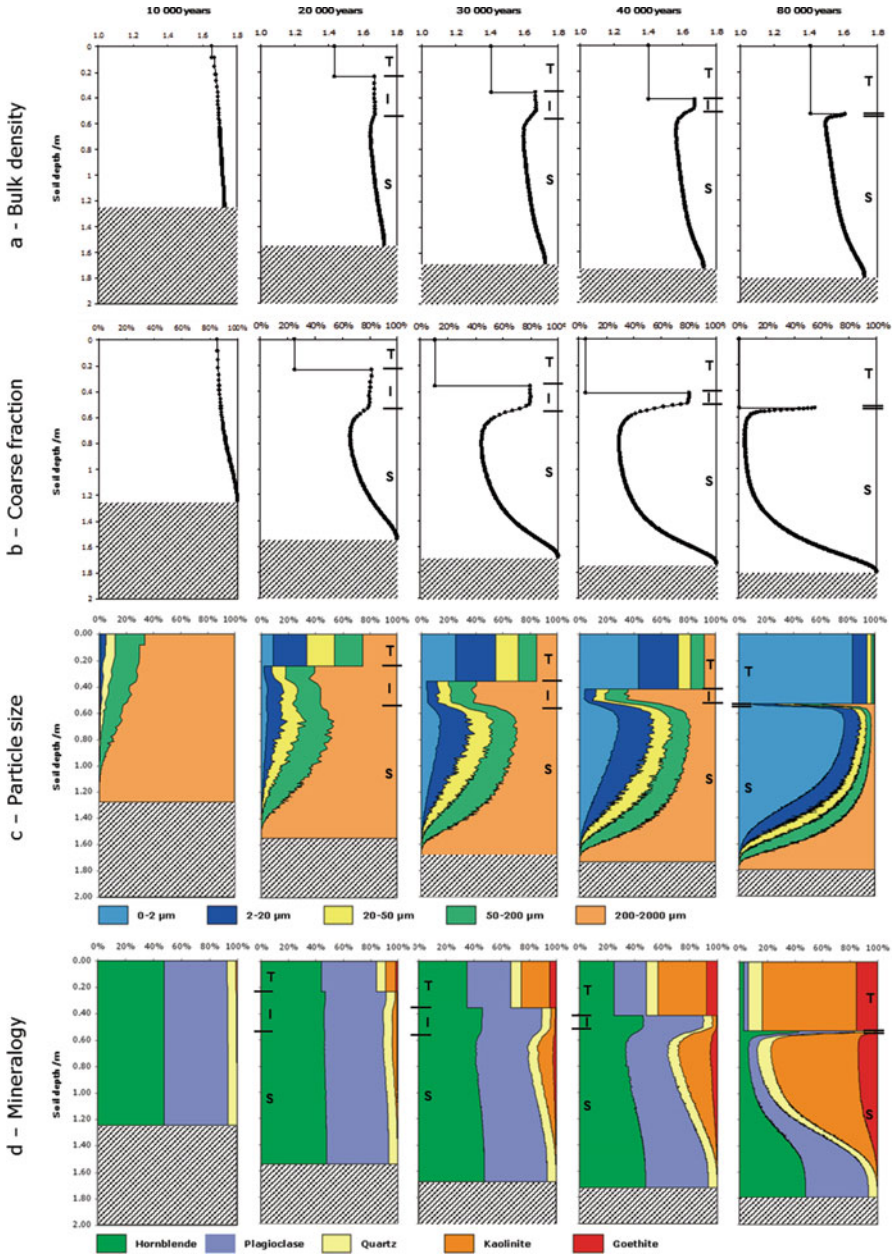


**Fig. 19.10** Example of the Pedogen model outputs: bulk density, coarse fraction, particle size and mineralogy in the soil profile after 10,000, 20,000, 30,000, 40,000 and 80,000 years (*T* topsoil, *I* intermediate, *S* subsoil horizon) (After Salvador-Blanes et al. 2007, used with permission)

### 19.2.2.1 Release of Regolith

The model is based on lowering rate of the bedrock surface that follows a negative exponential decline with increasing soil thickness (Minasny and McBratney 1999). Therefore, at each time step, a given quantity of regolith is released by the bedrock and constitutes a so-called layer with a given thickness. This layer is submitted at each subsequent time step to weathering, bioturbation and organic matter input and decay. The aim is here to follow the evolution of each layer; the sum of these layers constitutes the soil profile.

### 19.2.2.2 Physical Weathering of Coarse Fragments

The regolith released by the bedrock is considered to be made of spherical coarse fragments of a given size fraction. These rock grains, which are an assemblage of minerals, are considered to be submitted to physical weathering only, as the surface in contact with weathering agents is supposed to be negligible. The probability that fragments will break decreases with decreasing size, due to the fact that smaller particles contain fewer defects (Sharmeen and Willgoose 2006). Therefore, they break down to smaller fragments of various sizes according to first-order kinetic reactions. Once these fragments reach the size of 2 mm, they pertain to the fine fraction of the soil and are submitted to both physical and chemical weathering.

### 19.2.2.3 Physical and Chemical Weathering of the Fine Fraction

The intensity of physical and chemical weathering of the fine fraction is a function of the mineral type. For each of the defined layers, the fine fraction is divided into 1000 classes from 1000 to 1  $\mu\text{m}$  that correspond to the radius of the particles as they are considered spherical. This approach is similar to the one developed by Legros and Pedro (1985). All the individual mineral particles resulting from the physical fractionation of the coarse fraction are first considered to have an initial 1000  $\mu\text{m}$  radius.

The physical weathering of the fine fraction consists of the potential microdivision of a mineral into smaller particles. This microdivision is programmed as a conditional test based on the resistance of minerals to fractionation with a stochastic component. This resistance varies as well according to the size of the particle and its depth in the soil profile. The chemical weathering is assumed to consist in a congruent dissolution: the number of moles of a given mineral that are weathered is the product of its weathering rate constant and its surface area (White et al. 1996). The total surface area of the minerals corresponds here to the sum of the surface area of the spheres of a given mineral that compose a soil layer. Roughness and an internal porosity factor can be implemented to account for the nonspherical shape of the minerals, resulting in an underestimation of their surface area (White et al. 1996). To summarize, the quantity of the primary mineral that is weathered,



if relevant, the quantity of secondary minerals formed and finally the new radius of the weathered primary mineral and its redistribution in the relevant size class are calculated for each class, of each layer and at each time step.

#### 19.2.2.4 Bioturbation

The horizonation of in situ soil profiles results from translocation processes of soil material within the profile. Bioturbation is one of the processes that allows translocation of soil particles between horizons due to animals and plants (Hole 1981) and is addressed in this model. This process can be summarized as the homogenization of the topsoil and material transport between the subsoil and the topsoil (Müller-Lemans and van Dorp 1996). The amount of soil material translocated within the soil varies greatly according to several parameters. The model accounts for the maximum mass of soil translocated up and downwards, using data on surface casting (e.g. 1–5 kg m<sup>-2</sup> year<sup>-1</sup>, Paton et al. 1995), the coarse fragment content as a limiting factor to bioturbation and the position of the layer in the soil profile, as bioturbation rates decrease exponentially with depth in the soil.

#### 19.2.2.5 Organic Matter Dynamics

Further developments of the initial model have been made considering the organic matter dynamics (Salvador-Blanes et al. 2011). Organic matter dynamics are implemented through the application of a simple one-compartment model (Hémin and Dupuis 1945). Although simple, the model has, for example, been used for modelling the evolution of organic carbon contents at the landscape scale (Walter et al. 2003). This one-compartment model is moreover simple to use for time steps of the order of several decades to centuries. The input parameters to be addressed relate to input of fresh organic carbon to soil, organic carbon incorporation to the soil profile and mineralisation dynamics.

Fresh organic carbon input to soils depends on plant production that itself depends on climate and edaphic parameters. The annual input can therefore be approached by considering it equivalent to net primary productivity (NPP), for which many data exist in the literature. While vegetation is a buffer to the transfer of carbon from the atmosphere to the soil compartment, the model, with time steps of several decades to a century, allows to discard this issue. The simple global Miami model (Leith 1975) that links NPP to mean yearly temperature and rainfall has been used in Pedogen. Organic carbon production being strongly linked to soil moisture and nutrient availability, NPP values have been limited using soil available water content (AWC) as a proxy when rainfall is a limiting factor (annual potential evapotranspiration > rainfall), with threshold values equivalent to the approach in the TRIFFID model (Cox 2001). The soil AWC is calculated at each time step using a PTF linking field capacity and permanent wilting point to several soil properties.

The organic carbon incorporation to soil accounts for the root/shoot ratio ( $r/s$ ) and the input depth distribution in the soil profile. Constant averaged  $r/s$  values for given biomes are used (Jackson et al. 1996), according to the location of the modelled profile on the earth. The input depth distribution of organic carbon in the soil profile is correlated to the root depth distribution. This distribution varies according to the vegetation communities; it is modelled as a negative exponential decline with depth in the soil (Gale and Grigal 1987), according to the biome where the soil profile is located. Such an approach to constrain the input of OC according to soil depth in a numerical simulation of organic carbon dynamics has already been used by Elzein and Balesdent (1995). The mineralization dynamics is determined by using values of isohumic coefficients and mineralization rates given in the literature (Bayer et al. 2006).

#### 19.2.2.6 Strain

Several processes occur in the soil that lead to strain, e.g. a collapse or a dilation of the soil (increased weathering, bioturbation, arrangement of soil particles into pedes, incorporation of organic matter). This has in turn a consequence of the intensity of the processes modelled. To account for these changes, the bulk density of the layers in the soil profile is calculated at each time step according to one of the numerous bulk density PTFs available, which links bulk density to particle size properties, depth in the soil (Tranter et al. 2007).

Pedogen is a simple and ‘open’ model (additional processes can be incorporated), integrative of many complex pedogenetic processes, that requires few input parameters and can be adapted and implemented in a 2D/3D model as shown in the latter section of this chapter. Recent developments of this model, which incorporate the organic matter dynamics, allow an integration and interaction between processes with very different dynamics (physical and chemical weathering vs. bioturbation/organic matter), allowing to make a link with ecosystem modelling.

### 19.2.3 *The SoilGen Model*

Finke and Hutson (2008) followed by Finke (2012) devised a soil profile model called SoilGen. This model can be assimilated to a solute transport model that aims at simulating soil profile development over unconsolidated parent materials, accounting for factors of soil formation (Finke 2012). It is one of the few complete soil evolution models that simulates the changes in soil properties over millennium timescales, taking into account a wide range of processes (Opolot et al. 2015). As the processes occurring in the soil operate at very different timescales, they are modelled in SoilGen according to differing time steps (Finke and Hutson 2008; Finke 2012): milliseconds to hourly time steps (chemical and transport processes),

hourly time steps (heat flow and physical weathering), daily time steps (mineral weathering and organic matter dynamics) and yearly time steps (bioturbation, erosion/sedimentation and fertilization).

The description below is largely based on Opolot et al. (2015) that provides a complete summary of the SoilGen model, which was originally thoroughly described in Finke and Hutson (2008) and Finke (2012).

### 19.2.3.1 Water, Solute and Heat Transfer

Water, solute and heat transfers are based on the concepts of the LEACH-C code (Hutson 2003). The model solves the Richardson equation for the unsaturated vertical water flow, the convection/dispersion equation of the transfer of solutes and the heat flow equation for temperature distribution. Input parameters such as precipitation and evapotranspiration are corrected according to the local slope and exposition of the modelled profile.

### 19.2.3.2 Soil Chemical System and Chemical Equilibria

The model chemical system is divided into five phases: solution, precipitated, exchange, organic and unweathered phases. The input of ions to the solution is due to the dissolution of primary minerals, the decomposition of organic matter and external inputs through atmospheric deposition and fertilization. The removal of ions from the soil solution is due to plant uptake, leaching and precipitation. The equilibrium of the soil solution with precipitated and exchange phases is ensured by the application of several solubility laws and rate constants, with calculations at short time steps (Finke and Hutson 2008). The cations are adsorbed onto the solid phase by a Gapon exchange mechanism, and the exchange capacity is defined according to a regression equation combining organic carbon and clay contents, according to Foth and Ellis (1996), modified by a factor matching the initial CEC in the simulated pedon. However, the effect of pH on the CEC is not yet implemented.

### 19.2.3.3 Weathering Processes

Both physical and chemical weathering processes are described. Physical weathering processes are due to the strain caused by temperature gradients. The reduction in grain size is expressed by the probabilistic break-up of particles, as in Salvador-Blanes et al. (2007). Here, 12 size classes in the fine fraction (<2 mm) are considered. The probabilistic process is implemented as the splitting probability of a particle following a Bernoulli process according to the temperature gradient over a given time interval. However, this splitting process is restricted to fine, unconsolidated material. Chemical weathering is the major source of cations in nonagricultural soils. Here anorthite, chlorite, microcline and albite are considered

as major pools of  $\text{Ca}^{2+}$ ,  $\text{Mg}^{2+}$ ,  $\text{K}^{+}$  and  $\text{Na}^{+}$ , respectively. The weathering flux of each of these cations is defined as in Kros (2002) as a function of soil bulk density, the soil layer thickness, the volumic hydrogen concentration, a constant representing the effect of pH on the weathering rate and finally the content of the considered element in the primary mineral. The weathering flux of Al is determined considering a congruent weathering of the aforementioned minerals.

#### **19.2.3.4 Vegetation, Carbon Cycling and Plant Uptake Processes**

SoilGen allows the interaction between the soil and the vegetation through annual litter input, carbon cycling and ion uptake, according to four vegetation types (grass/scrub, agriculture, conifers, deciduous wood) (Finke and Hutson 2008). The carbon cycling is simulated according to the RothC-26.3 model (Jenkinson and Coleman 1994).

#### **19.2.3.5 Soil Phase Redistribution Processes**

Solid phase redistribution processes are considered through several aspects. The clay migration process is extensively described in the model, combining detachment, dispersion, transportation and deposition processes. The detachment process occurs at the soil surface through the impact of raindrops and is modelled according to Jarvis et al. (1999) modified by Finke (2012). The dispersion process is described both at the surface and within the soil profile, when the solute concentration decreases below a threshold value. Finally, the filtering process, defined as the entrapment of clay particles in small pores, is based on calculated pore water velocities. The bioturbation process is described as an incomplete mixing process, whereas tillage is considered as an extreme bioturbation process within the surface of the soil profile (Finke and Hutson 2008). Other processes, such as erosion or sedimentation, which result in the addition or removal of soil material at the surface of the soil profile and dissolution and precipitation of calcite and gypsum are described as well. However, the collapse and/or dilation through these various processes are not accounted for in the model.

#### **19.2.3.6 Applications of the SoilGen Model**

Successful applications of the SoilGen model have been performed, both at the profile and at the landscape scale. At the profile scale, the model was initially implemented to demonstrate its ability to simulate the effect of climate/vegetation/organisms on the soil formation on calcareous loess in Belgium and Hungary (Finke and Hutson 2008). Further developments of the model allowed to test its sensitivity to historic climatic fluctuations in different topographic conditions over a similar parent material (Finke 2012). A quality test of the

model was performed on soil chronosequences developed in marine sediments in Norway (Sauer et al. 2012), which showed that the model fitted well for some soil properties such as particle size distribution, but underestimated some other properties. Discrepancies were analysed, and possible improvements of the model were suggested, such as the description of soil structure formation. At the landscape scale, the model was applied over 96 soil profiles disseminated over 584 km<sup>2</sup> in Northern Belgium (Zwertvaegher et al. (2013)). This application allowed to reconstruct soil characteristics (texture, bulk density, organic carbon, calcite content, pH) that fitted well with the current properties and allowed to reconstruct soil characteristic maps at specific points in the past. Finally, the model was applied over 108 soil profiles to test the possible effect of tree uprooting on some soil properties (Finke et al. 2014). The simulations, coupled with regression kriging, allowed to prove that tree uprooting is an important process determining horizon thicknesses.

The SoilGen model is probably the most complete integrated soil profile model to date. It has been tested both at the pedon and landscape scales and confronted to actual soil properties, with good matches for some soil properties and some discrepancies for others. Further developments include the extension to additional primary minerals and elements, to the formation of secondary minerals and to the further development of the interactions between soil and vegetation (Opolot et al. 2015).

## 19.3 Soil-Landscape Models

### 19.3.1 *Soil-Landscape Models*

Recent developments in process modelling focus on mechanistic simulations of soil formation in the landscape based on the principals of mass balance. Huggett's (1975) homomorphic modelling approach can perhaps be regarded as the first representation of soil-landscape evolution modelling. Huggett (1975) proposed to model the evolution of a soil system in a three-dimensional way on the catena scale over millennial timescales, considering also the formation of soil horizons over time. He explained further that concaving contours in a downslope direction should lead to convergent flow lines whereas convex contours should lead to divergent flow lines and that all flow lines should converge in hollows and diverge over spurs. All 'flowlines' should then join in one complex network, based on first- and second-order streamlines.

The simplest model of soil-landscape evolution that has been formulated implements the change in elevation as a function of material transport (Stockmann et al. 2011):

$$\frac{\partial z}{\partial t} = -\nabla q_s \quad (19.16)$$

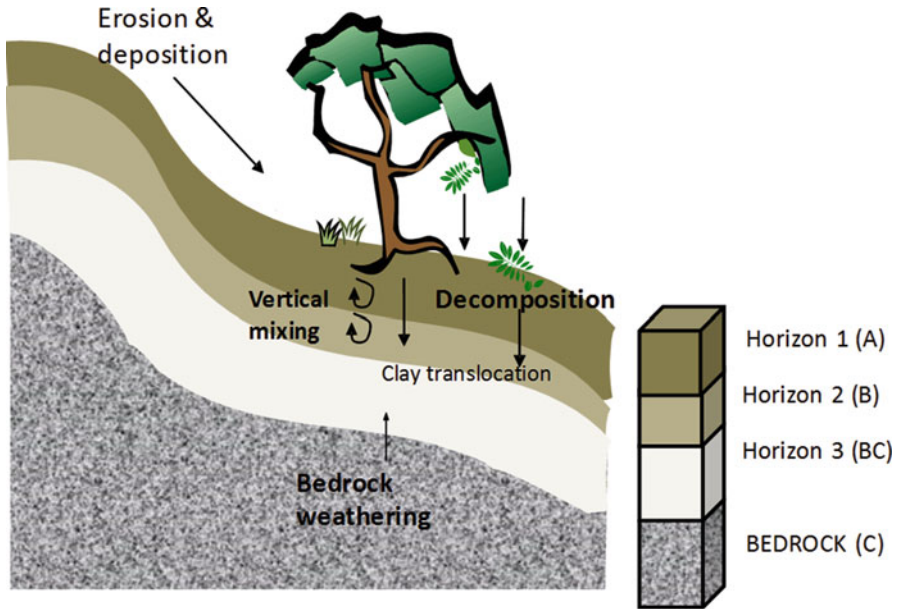


Fig. 19.11 Schematic representation of a simple soil-landscape model

where  $z$  is the elevation,  $t$  is time,  $q_s$  is the material flux and  $\nabla$  is a partial derivative vector. Dietrich et al. (1995) and later Heimsath et al. (1997) introduced soil into the continuity equation of mass transport along a hillslope (Eq. 19.16):

$$\rho_s \frac{\partial h}{\partial t} = -\rho_r \frac{\partial e}{\partial t} - \nabla q_s \quad (19.17)$$

where  $h$  is soil thickness,  $\rho_s$  and  $\rho_r$  are the bulk densities of soil and rocks,  $e$  is the elevation of the bedrock-soil interface,  $t$  is time and  $q_s$  is the material flux in the horizontal direction (Fig. 19.11).

Minasny and McBratney (1999) and following on Minasny and McBratney (2001) used some of the basic concepts described in Huggett (1975) and Heimsath et al. (1997) to introduce a two-dimensional rudimentary mechanistic pedogenetic model. Based on a digital elevation model (DEM), pedogenesis is simulated by a combination of several sub-models: (1) physical weathering starting from bedrock employing the rate of exponential decline of soil production with increasing soil thickness, (2) chemical weathering represented as a negative exponential function of both soil thickness and time and (3) movement of soil material as characterized by a diffusion transport model. The upscaling result of such an analysis is illustrated in Fig. 19.12, whereby, after 10,000 years, soil accumulation is predominant in the gullies compared with the ridges, where soil erodes.

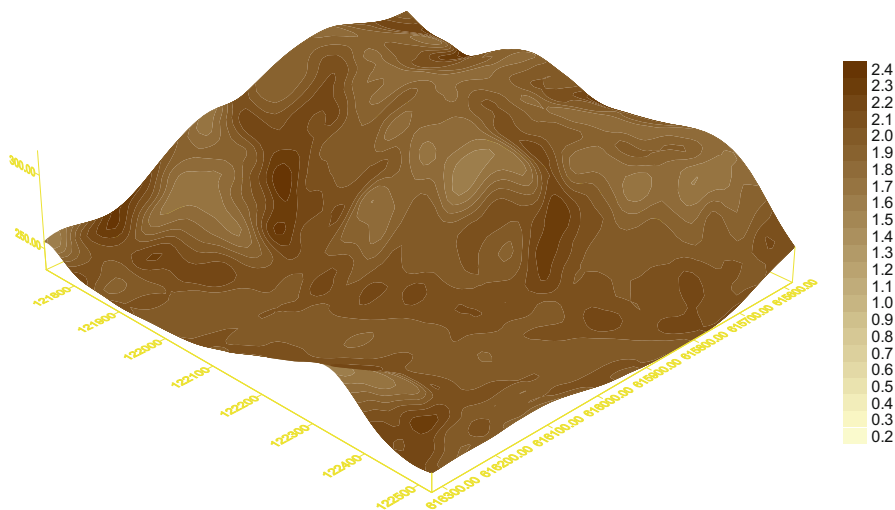


**Fig. 19.12** Simulated soil formation in a landscape after 10,000 years, shading represents soil thickness (*m*) (After Minasny and McBratney 2001)

### 19.3.2 *Linking Landscape-Scale Models and Soil Profile-Scale Models*

While current soil models allow a detailed simulation at the profile level as discussed in Sect. 19.2, they lack horizontal integration, with models from the geomorphology community, where the most advanced LEMs include a wide array of erosion processes and accurate description of erosion-deposition processes, but lack attention to vertical soil formation processes.

One of the first attempts to such an integrated model was the model for integrated soil development (MILESD) by Vanwalleghem et al. (2013). MILESD is a four-layer model with five texture classes. It includes the main soil-forming processes: physical weathering, chemical weathering, clay migration and neoformation, bioturbation and carbon cycling. Landscape evolution is represented by concentrated flow erosion and creep, allowing for selective transport and deposition and with negative feedbacks from stoniness and vegetation on the erosion rates. The model was developed so that soil formation and evolution could be modelled with enough detail while at the same time reducing runtime to allow landscape-scale simulations. Potential drawbacks of this simplified approach include the fact that the soil solution and soil chemistry are not included explicitly. Therefore, all soil-forming processes need to be calibrated on a site-specific basis.

Vanwalleghem et al. (2013) applied MILESD to a 6.25 km<sup>2</sup> study area in Werrikimbe National Park (NSW, Australia) where it was validated against field profile data (Fig. 19.13). The results showed that trends in soil thickness were

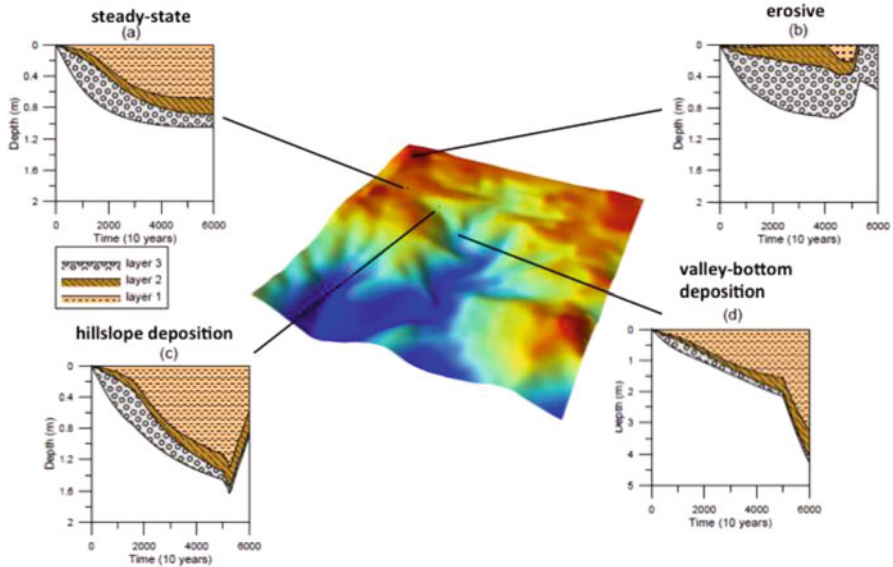


**Fig. 19.13** Evolution of soil horizons in four different landscape positions, from erosive over stable (steady-state) to depositional for a constant erosion rate during the first 50,000 years followed by higher erosion period during the last 10,000 years

predicted well along a catena. Soil texture and bulk density could be predicted reasonably well, with errors in the order of 10%. Figure 19.13 clearly shows the potential of these types of integrated models. The evolution of soil horizons over time is shown for different positions in the landscape, ranging from erosive over stable to depositional. The results show a model run to 60,000 years where a constant erosion rate was followed by a higher erosion rate during the last 10,000 years. It can be seen how important differences along the catena emerge with a stable soil profile on the plateau (a), an erosive hillslope where the top two horizons disappear altogether (b), a hillslope deposition site that eventually erodes when erosion rates increase at the end of the simulation (c) and a deep depositional soil in the valley bottom (d).

Figure 19.14 shows the result of soil formation-erosion interactions on the organization and evolution of soil properties in the entire catchment. Increasing erosion rate and increasing age of the landscape both lead to an increase in semivariance, which implies a higher spatial variability over time. In this particular context, it seems that erosion and deposition are key drivers of soilscape heterogeneity as the semivariogram responds strongly to increasing erosion rates.

Temme and Vanwalleghem (2016) presented a new soil-landscape model, called LORICA, that integrated MILESD with the existing landscape evolution model LAPSUS. The coupling with a more advanced landscape evolution model allows taking into account different erosion processes, e.g. landsliding, which improves the applicability of the soilscape model to a wider range of environments. With respect



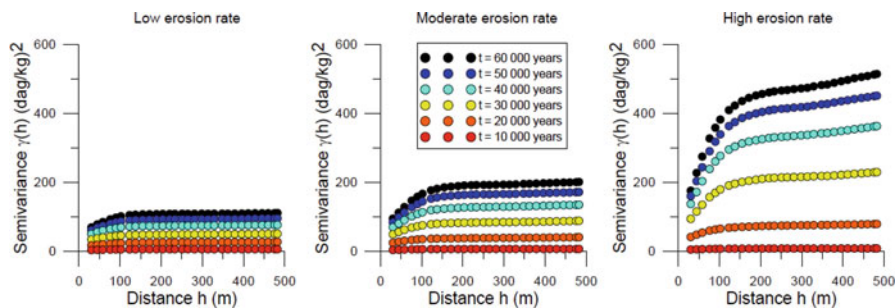


**Fig. 19.14** Evolution of the spatial variability of clay content in topsoil (0–0.2 m) as a function of time and erosion rate. Erosion rate increases from left to right

to the representation of soil genesis, the main novelty is the elimination of the fixed layer limitation. LORICA uses an advanced multilayer approach, where new layers are generated or existing layers are joined on a need-be basis. van der Meij et al. (2015) applied LORICA to simulate the development of Arctic soils, which allowed to single out the importance of aeolian deposition.

Another suite of advanced, fully three-dimensional soilscape models was developed by Cohen et al. (2010, 2015) and Welivitiya et al. (2016). Both mARM3D (Cohen et al. 2010) and its extension, mARM5D (Cohen et al. 2015), simulate the evolution of soil particle size distribution via physical weathering, profile depth as a function of weathering, aeolian deposition and diffusive and fluvial sediment transport. With the model SSSPAM, the latest version in this model family, Welivitiya et al. (2016) performed an extensive sensitivity analysis, generalizing the physical dependence of the relationship between contributing area, local slope, and the surface soil particle size distribution.

It is clear from the previous discussion that the existing soilscape models will need to be developed and tested further. The issue of the ideal number of soil horizons to consider is not trivial. Although, ideally, an infinite number of horizons assure a full representation of the profile's complexity, increasing the number of horizons in any model will imply increasing computation time significantly. Moreover, soil scientists often record field data with a number of limited soil horizons. This implies that in a validation exercise, the results of a model with many horizons have to be 'converted back' into a profile with less horizons. To that extent, the four-layer approach of the simple MILESD model corresponds to the way soil profiles are described in the field. Several processes are currently represented poorly or not at all in soilscape models. Soil chemical weathering is probably the most critical process that is currently represented in an overly simplified manner. Several studies, both in the laboratory (e.g. Maher 2010) and in field conditions (e.g. Schoonejans et al. 2016), have shown the dependency of chemical weathering on soil hydrological fluxes. Pore water dynamics are currently not explicitly represented in soilscape models. This limitation could be solved by coupling more detailed point-based models, such as SoilGen, to landscape evolution

models, as proposed by Opolot et al. (2015). This would be increasingly beneficial in terms of computational resources in landscapes where landscape evolution is several orders of magnitude faster compared to soil formation processes or vice versa, and the exchange of input-output data between models is not necessary during every model time step.

So clearly, much work is required to better model the effect of climate and organisms on the soil's chemistry, mineralogy, physics and biology (Chadwick et al. 2003). It is also essential to integrate soil processes, which are usually only represented at a profile scale, with landscape processes (Viaud et al. 2010).

## References

- Ahnert F (1977) Some comments on the quantitative formulation of geomorphological processes in a theoretical model. *Earth Surface Processes* 2:191–201
- Aitken MJ (1998) An introduction to optical dating. The dating of quaternary sediments by the use of photon-stimulated luminescence. Oxford University Press, Oxford
- Barrett LR, Schaetzl RJ (1992) An examination of podzolization near Lake Michigan using chronofunctions. *Can J Soil Sci* 72:527–541
- Bayer C, Lovato T, Dieckow J, Zanatta JA, Mielniczuk J (2006) A method for estimating coefficients of soil organic matter dynamics based on long-term experiments. *Soil Tillage Res* 91:217–226
- Brantley SL, Megonigal JP, Scatena FN, Balogh-Brunstad Z, Barnes RT, Bruns MA, Van Cappellen P, Dontsova K, Hartnett HE, Hartshorn AS, Heimsath A, Herndon E, Jin L, Keller CK, Leake JR, McDowell WH, Meinzer FC, Mozdzer TJ, Petsch S, Pett-Ridge J, Pregitzer KS, Raymond PA, Riebe C, Shumaker S, Sutton-Grier A, Walter R, Yoo K (2011) Twelve testable hypotheses on the geobiology of weathering. *Geobiology* 9:140–165
- Brimhall GH, Dietrich WE (1987) Constitutive mass balance relations between chemical composition, volume, density, porosity, and strain in metasomatic hydrochemical systems: results on weathering and pedogenesis. *Geochim Cosmochim Acta* 51:567–587
- Burke BC, Heimsath AM, White AF (2007) Coupling chemical weathering with soil production across soil-mantled landscapes. *Earth Surf Process Landf* 32:853–873
- Burke BC, Heimsath AM, Dixon JL, Chappell J, Yoo K (2009) Weathering the escarpment: chemical and physical rates and processes, south-eastern Australia. *Earth Surf Process Landf* 34:768–785
- Chadwick OA, Gavenda RT, Kelly EF, Ziegler K, Olson CG, Elliott WC, Hendricks DM (2003) The impact of climate on the biogeochemical functioning of volcanic soils. *Chem Geol* 202:195–223
- Chmeleff J, von Blanckenburg F, Kossert K, Jakob D (2009) Determination of the  $^{10}\text{Be}$  half-life by multi collector ICP-mass spectrometry and liquid scintillation counting. *Goldschmidt abstracts 2009 – C. Geochim Cosmochim Acta* 73:A221–A221
- Cohen S, Willgoose G, Hancock G (2010) The mARM3D spatially distributed soil evolution model: three-dimensional model framework and analysis of hillslope and landform responses. *J Geophys Res Earth* 115:F04013
- Cohen S, Willgoose G, Svoray T, Hancock G, Sela S (2015) The effects of sediment transport, weathering, and aeolian mechanisms on soil evolution. *J Geophys Res Earth* 120:260–274
- Cox P (2001) Description of the “TRIFFID” dynamic global vegetation model. Technical note 24. Hadley Centre, Met Office, London
- Dietrich WE, Reiss R, Hsu M-L, Montgomery DR (1995) A process-based model for colluvial soil depth and shallow landsliding using digital elevation data. *Hydrol Process* 9:383–400

- Dijkerman JC (1974) Pedology as a science: the role of data, models and theories in the study of natural soil systems. *Geoderma* 11:73–93
- Dixon JL, Heimsath AM, Amundson R (2009) The critical role of climate and saprolite weathering in landscape evolution. *Earth Surf Process Landf* 34:1507–1521
- Dörr H (1995) Application of  $^{210}\text{Pb}$  in soils. *J Paleolimnol* 13:157–168
- Dosseto A, Turner SP, Chappell J (2008) The evolution of weathering profiles through time: new insights from uranium-series isotopes. *Earth Planet Sci Lett* 274:359–371
- Dunne J, Elmore D, Muzikar P (1999) Scaling factors for the rates of production of cosmogenic nuclides for geometric shielding and attenuation at depth on sloped surfaces. *Geomorphology* 27:3–11
- Egli M, Dahms D, Norton K (2014) Soil formation rates on silicate parent material in alpine environments: different approaches-different results? *Geoderma* 213:320–333
- Elzein A, Balesdent J (1995) Mechanistic simulation of vertical distribution of carbon concentrations and residence times in soils. *Soil Sci Soc Am J* 59:1328–1335
- Finke PA (2012) Modeling the genesis of Luvisols as a function of topographic position in loess parent material. *Quat Int* 265:3–17
- Finke PA, Hutson JL (2008) Modelling soil genesis in calcareous loess. *Geoderma* 145:462–479
- Finke PA, Vanwalleghem T, Opolot E, Poesen J, Deckers J (2014) Estimating the effect of tree uprooting on variation of soil horizon depth by confronting pedogenetic simulations to measurements in a Belgian loess area. *J Geophys Res-Earth Surf* 118:1–16
- Foth HD, Ellis BG (1996) *Soil fertility*, 2nd edn. CRC Press, Lewis
- Furbish DJ, Fagherazzi S (2001) Stability of creeping soil and implications for hillslope evolution. *Water Resour Res* 37:2607–2618
- Gabet EJ, Mudd SM (2010) Bedrock erosion by root fracture and tree throw: a coupled biogeomorphic model to explore the humped soil production function and the persistence of hillslope soils. *J Geophys Res Earth* 115:F04005
- Gabet EJ, Reichman OJ, Seabloom EW (2003) The effects of bioturbation on soil processes and sediment transport. *Annu Rev Earth Planet Sci* 31:249–274
- Gale MR, Grigal DF (1987) Vertical root distributions of northern tree species in relation to successional status. *Can J For Res* 17:829–834
- Gilbert GK (1877) Report on the geology of the Henry Mountains (Utah). United States Geological Survey, Washington, DC
- Granger DE, Muzikar PF (2001) Dating sediment burial with in situ-produced cosmogenic nuclides: theory, techniques, and limitations. *Earth Planet Sci Lett* 188:269–281
- Green EG, Dietrich WE, Banfield JF (2006) Quantification of chemical weathering rates across an actively eroding hillslope. *Earth Planet Sci Lett* 242:155–169
- Hay RL (1960) Rate of clay formation and mineral alteration in a 4000-year-old volcanic ash soil on St. Vincent, B.W.I. *Am J Sci* 258:354–368
- He Q, Walling DE (1996) Interpreting particle size effects in the adsorption of  $^{137}\text{Cs}$  and unsupported  $^{210}\text{Pb}$  by mineral soils and sediments. *J Environ Radioact* 30:117–137
- Heimsath AM, Dietrich WE, Nishiizumi K, Finkel RC (1997) The soil production function and landscape equilibrium. *Nature* 388:358–361
- Heimsath AM, Dietrich WE, Nishiizumi K, Finkel RC (1999) Cosmogenic nuclides, topography, and the spatial variation of soil depth. *Geomorphology* 27:151–172
- Heimsath AM, Fink D, Hancock GR (2009) The ‘humped’ soil production function: eroding Arnhem Land, Australia. *Earth Surf Process Landf* 34:1674–1684
- Hénin S, Dupuis M (1945) Essai de bilan de la matière organique du sol. *Ann Agronomiques* 11:17–29
- Heuvelink GBM, Webster R (2001) Modelling soil variation: past, present and future. *Geoderma* 100:269–301
- Hole FD (1981) Effects of animals on soil. *Geoderma* 25:75–112
- Hoosbeek MR (1994) Towards the quantitative modeling of pedogenesis: a review – reply – pedology beyond the soil-landscape paradigm: pedodynamics and the connection to other sciences. *Geoderma* 63:303–307

- Huggett RJ (1975) Soil landscape systems: a model of soil genesis. *Geoderma* 13:1–22
- Huggett RJ (1998) Soil chronosequences, soil development, and soil evolution: a critical review. *Catena* 32:155–172
- Humphreys GS, Wilkinson MT (2007) The soil production function: a brief history and its rediscovery. *Geoderma* 139:73–78
- Hutson JL (2003) LEACHM e a process-based model of water and solute movement, transformations, plant uptake and chemical reactions in the unsaturated zone. Version 4. Research series no R03-1 (Dept. of Crop and Soil Sciences, Cornell University, Ithaca, NY). *J Soil Sci* 36:97–121
- Jackson RB, Canadell J, Ehleringer JR, Mooney HA, Sala OE, Schulze ED (1996) A global analysis of root distributions for terrestrial biomes. *Oecologia* 108:389–411
- Jagercikova M, Evrard O, Balesdent J, Lefèvre I, Cornu S (2014) Modeling the migration of fallout radionuclides to quantify the contemporary transfer of fine particles in Luvisol profiles under different land uses and farming practices. *Soil Tillage Res* 140:82–97
- Jarvis NJ, Villholth KG, Ulén B (1999) Modelling particle mobilization and leaching in macroporous soil. *Eur J Soil Sci* 50:621–632
- Jenkinson DS, Coleman K (1994) Calculating the annual input of organic matter to soil from measurements of total organic carbon and radiocarbon. *Eur J Soil Sci* 45:167–174
- Jenny H (1941) Factors of soil formation. A system of quantitative pedology. McGraw-Hill Book Company, New York
- Kaste JM, Heimsath AM, Bostick BC (2007) Short-term soil mixing quantified with fallout radionuclides. *Geology* 35:243–246
- Kirkby MJ (1977) Soil development models as a component of slope models. *Earth Surface Process* 2:203–230
- Kirkby MJ (1985) A basis for soil profile modelling in a geomorphic context. *J Soil Sci* 36:97–121
- Kitayama K, Edward AGS, Drake DR, Mueller-Dombois D (1997a) Fate of a wet montane forest during soil ageing in Hawaii. *J Ecol* 85:669–679
- Kitayama K, Schuur EAG, Drake DR, Mueller-Dombois D (1997b) Fate of a wet montane forest during soil ageing in Hawaii. *J Ecol* 85:669–679
- Kros J (2002) Evaluation of biogeochemical models at local and regional scale. PhD thesis. Wageningen University, Wageningen, The Netherlands
- Lal D (1991) Cosmic ray labeling of erosion surfaces: in situ nuclide production rates and erosion models. *Earth Planet Sci Lett* 104:424–439
- Larsen IJ, Almond PC, Eger A, Stone JO, Montgomery DR, Malcolm B (2014) Rapid soil production and weathering in the southern alps, New Zealand. *Science* 343:637–640
- Legros JP, Pedro G (1985) The causes of particle-size distribution in soil profiles derived from crystalline rocks, France. *Geoderma* 36:15–25
- Leith H (1975) Modelling the primary productivity of the world. In: Leith H, Whittaker RH (eds) Primary productivity of the biosphere. Springer-Verlag, Berlin
- Levine ER, Knox RG (1994) A comprehensive framework for modeling soil genesis. In: Bryant RB, Arnold RW (eds) Quantitative modeling of soil forming processes. Soil Science Society of America, Madison, pp 77–89. SSSA Special Publication No 39
- Ludwig W, Probst JL (1998) River sediment discharge to the oceans: present-day controls and global budget. *Am J Sci* 298:265–295
- Mabit L, Benmansour M, Walling DE (2008) Comparative advantages and limitations of the fallout radionuclides  $^{137}\text{Cs}$ ,  $^{210}\text{Pb}_{\text{ex}}$  and  $^7\text{Be}$  for assessing soil erosion and sedimentation. *J Environ Radioact* 99:1799–1807
- Maher K (2010) The dependence of chemical weathering rates on fluid residence time. *Earth Planet Sci Lett* 294:101–110
- Minasny B, McBratney AB (1999) A rudimentary mechanistic model for soil production and landscape development. *Geoderma* 90:3–21
- Minasny B, McBratney AB (2001) A rudimentary mechanistic model for soil production and landscape development II. A two-dimensional model incorporating chemical weathering. *Geoderma* 103:161–179

- Minasny B, McBratney AB (2006) Mechanistic soil-landscape modelling as an approach to developing pedogenetic classifications. *Geoderma* 133:138–149
- Minasny B, Finke P, Stockmann U, Vanwallegem T, McBratney AB (2015) Resolving the integral connection between pedogenesis and landscape evolution. *Earth Sci Rev* 150:102–120
- Montgomery DR (2007) Soil erosion and agricultural sustainability. *Proc Natl Acad Sci* 104:13268–13272
- Müller-Lemans H, van Dorp F (1996) Bioturbation as a mechanism for radionuclide transport in soil: relevance of earthworms. *J Environ Radioact* 31:7–20
- Nishiizumi K, Kohl CP, Arnold JR, Klein J, Fink D, Middleton R (1991) Cosmic ray produced  $^{10}\text{Be}$  and  $^{26}\text{Al}$  in Antarctic rocks: exposure and erosion history. *Earth Planet Sci Lett* 104:440–454
- NRC (2010) Landscapes on the edge. New horizons for research on Earth's surface. The National Academy Press, Washington, DC
- Opolot E, Yu YY, Finke PA (2015) Modeling soil genesis at pedon and landscape scales: achievements and problems. *Quat Int* 376:34–46
- Oreskes N, Shrader-Frechette K, Belitz K (1994) Verification, validation and confirmation of numerical models in the earth sciences. *Science* 263:641–646
- Paton TR, Humphreys GS, Mitchell PB (1995) Soils: a new global view. University College London Press, London
- Portenga EW, Bierman PR (2011) Understanding Earth's eroding surface with  $^{10}\text{Be}$ . *GSA Today* 21:4–10
- Riebe CS, Kirchner JW, Finkel RC (2003) Long-term rates of chemical weathering and physical erosion from cosmogenic nuclides and geochemical mass balance. *Geochim Cosmochim Acta* 67:4411–4427
- Riebe CS, Kirchner JW, Finkel RC (2004a) Erosional and climatic effects on long-term chemical weathering rates in granitic landscapes spanning diverse climate regimes. *Earth Planet Sci Lett* 224:547–562
- Riebe CS, Kirchner JW, Finkel RC (2004b) Sharp decrease in long-term chemical weathering rates along an altitudinal transect. *Earth Planet Sci Lett* 218:421–434
- Salvador-Blanes S, Minasny B, McBratney AB (2007) Modelling long term in-situ soil profile evolution – application to the genesis of soil profiles containing stone layers. *Eur J Soil Sci* 58:1535–1548
- Salvador-Blanes S, Minasny B, McBratney AB (2011) Modelling soil formation at the profile scale. European Geosciences Union General Assembly 2011. *Geophys Res Abstr* 13:EGU2011–EG13012
- Sauer D, Schellmann G, Stahr K (2007) A soil chronosequence in the semi-arid environment of Patagonia (Argentina). *Catena* 71:382–393
- Sauer D, Finke PA, Schüllli-Maurer I, Sperstad R, Sørensen R, Høeg HI, Stahr K (2012) Testing a soil development model against southern Norway soil chronosequences. *Quat Int* 265:18–31
- Schaetzl RJ, Barrett LR, Winkler JA (1994) Choosing models for soil chronofunctions and fitting them to data. *Eur J Soil Sci* 45:219–232
- Schoonejans J, Vanacker V, Opfergelt S, Ameijeiras-Mariño Y, Christl M (2016) Kinetically limited weathering at low denudation rates in semiarid climatic conditions. *J Geophys Res Earth* 121:336–350
- Sharmeen S, Willgoose GR (2006) The interaction between armouring and particle weathering for eroding landscapes. *Earth Surf Process Landf* 31:1195–1210
- Shouse M, Phillips J (2016) Soil deepening by trees and the effects of parent material. *Geomorphology* 269:1–7
- Sommer M, Gerke HH, Deumlich D (2008) Modelling soil landscape genesis: a “time split” approach for hummocky agricultural landscapes. *Geoderma* 145:480–493
- Sparks DL (1995) 7 – Kinetics of soil chemical processes. *Environmental soil chemistry*. Academic, Boston, pp 159–185
- Stevens PR, Walker TW (1970) The chronosequence concept and soil formation. *Q Rev Biol* 45:333–350

- Stockmann U (2010) Quantifying processes of pedogenesis. A field study situated in the Werrikimbe National Park in south-eastern Australia. Faculty of Agriculture, Food and Natural Resources. The University of Sydney, p 234
- Stockmann U, Minasny B, McBratney A (2011) Quantifying processes of pedogenesis. *Adv Agron* 113:1–74
- Stockmann U, Minasny B, Pietsch TJ, McBratney AB (2013) Quantifying processes of pedogenesis using optically stimulated luminescence. *Eur J Soil Sci* 64:145–160
- Stockmann U, Minasny B, McBratney AB (2014) How fast does soil grow? *Geoderma* 216:48–61
- Stone JO (2000) Air pressure and cosmogenic isotope production. *J Geophys Res* 105:23,753–723,759
- Suresh PO, Dosseto A, Hesse PP, Handley HK (2013) Soil formation rates determined from uranium-series isotope disequilibria in soil profiles from the southeastern Australian highlands. *Earth Planet Sci Lett* 379:26–37
- Sverdrup H, Warfvinge P (1993) Calculating field weathering rates using a mechanistic geochemical model – profile. *Appl Geochem* 8:273–283
- Syvitski JPM, Vorosmarty CJ, Kettner AJ, Green P (2005) Impact of humans on the flux of terrestrial sediment to the global coastal ocean. *Science* 308:376–380
- Temme AJAM, Vanwallegem T (2016) LORICA – a new model for linking landscape and soil profile evolution: development and sensitivity analysis. *Comput Geosci* 90(Part B):131–143
- Tranter G, Minasny B, McBratney AB, Murphy B, McKenzie NJ, Grundy M (2007) Building and testing conceptual and empirical models for predicting soil bulk density. *Soil Use Manag* 23:437–443
- van der Meij WM, Temme AJAM, de Kleijn CMFJJ, Reimann T, Heuvelink GBM, Zwoliński Z, Rachlewicz G, Rymer K, Sommer M (2015) Arctic soil development on a series of marine terraces on Central Spitsbergen, Svalbard: a combined geochronology, fieldwork and modelling approach. *SOIL Discuss* 2015:1345–1391
- Van Wambeke A (1972) Mathematical expression of eluviation-illuviation processes and the computation of the effects of clay migration in homogeneous soil parent materials. *J Soil Sci* 23:325–332
- Van Wambeke A (1976) A mathematical model for the differential movement of two soil constituents into illuvial horizons: application to clay ratios in argillic horizons. *J Soil Sci* 27:111–120
- Vanwallegem T, Stockmann U, Minasny B, McBratney AB (2013) A quantitative model for integrating landscape evolution and soil formation. *J Geophys Res Earth* 118:1–17
- Viaud V, Angers DA, Walter C (2010) Towards landscape-scale modeling of soil organic matter dynamics in agroecosystems. *Soil Sci Soc Am J* 74:1–14
- Wagenet RJ, Hutson JL, Bouma J (1994) Modeling water and chemical fluxes as driving forces of pedogenesis. In: Bryant RB, Arnold RW (eds) *Quantitative modeling of soil forming processes*. Soil Science Society of America, Madison, pp 17–35. SSSA Special Publication No 39
- Walter C, Viscarra-Rossel RA, McBratney AB (2003) Spatio-temporal simulation of the field-scale evolution of organic carbon over the landscape. *Soil Sci Soc Am J* 67:1477–1486
- Welivitiya WDDP, Willgoose GR, Hancock GR, Cohen S (2016) Exploring the sensitivity on a soil area-slope-grading relationship to changes in process parameters using a pedogenesis model. *Earth Surf Dynam Discuss* 2016:1–43
- Wells T, Willgoose GR, Hancock GR (2008) Modeling weathering pathways and processes of the fragmentation of salt weathered quartz-chlorite schist. *J Geophys Res Earth* 113:F01014
- White AF, Blum AE (1995) Effects of climate on chemical weathering in watersheds. *Geochim Cosmochim Acta* 59:1729–1747

- White AF, Blum AE, Schulz MS, Bullen TD, Harden JW, Peterson ML (1996) Chemical weathering rates of a soil chronosequence on granitic alluvium: I. Quantification of mineralogical and surface area changes and calculation of primary silicate reaction rates. *Geochim Cosmochim Acta* 60:2533–2550
- Wilkinson MT, Humphreys GS (2005) Exploring pedogenesis via nuclide-based soil production rates and OSL-based bioturbation rates. *Aust J Soil Res* 43:767–779
- Wilkinson BH, McElroy BJ (2007) The impact of humans on continental erosion and sedimentation. *Geol Soc Am Bull* 119:140–156
- Yaalon DH (1975) Conceptual models in pedogenesis: can soil-forming functions be solved? *Geoderma* 14:189–205
- Yoo K, Amundson R, Heimsath AM, Dietrich WE, Brimhall GH (2007) Integration of geochemical mass balance with sediment transport to calculate rates of soil chemical weathering and transport on hillslopes. *J Geophys Res* 112:1–15
- Zapata F (2003) The use of environmental radionuclides as tracers in soil erosion and sedimentation investigations: recent advances and future developments. *Soil Tillage Res* 69:3–13
- Zwertvaegher A, Finke P, De Smedt P, Gelorini V, Van Meirvenne M, Bats M, De Reu J, Antrop M, Bourgeois J, De Maeyer P, Verniers J, Crombe P (2013) Spatio-temporal modeling of soil characteristics for soilscape reconstruction. *Geoderma* 207–208:166–179